Supplementary figures and legends

Suppl. Figure 1

a.

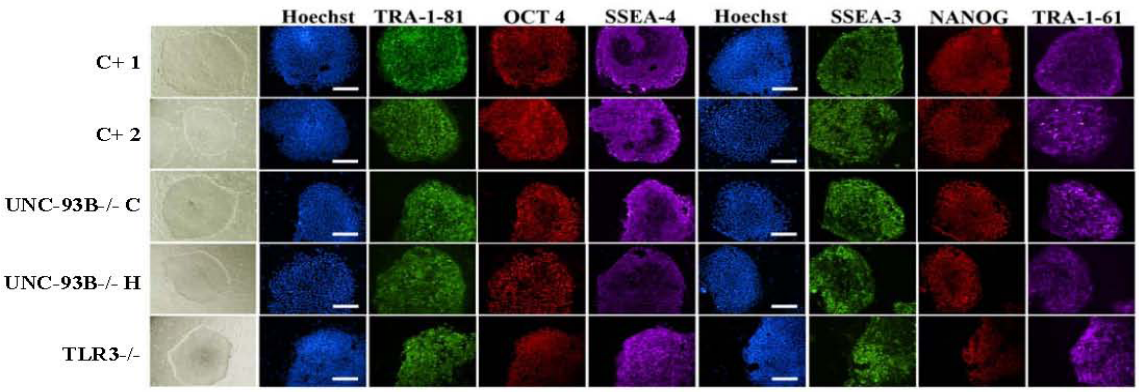

b.

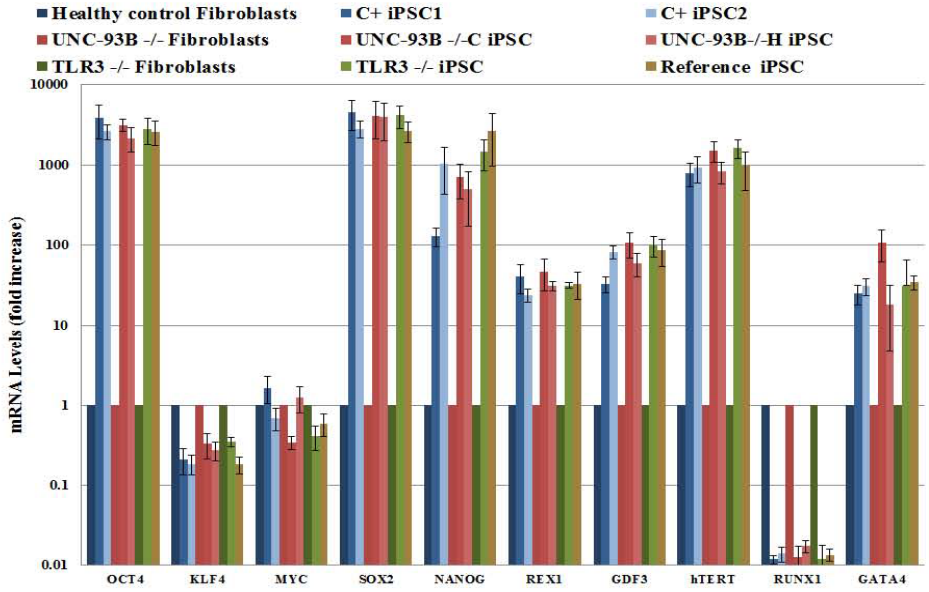

c.

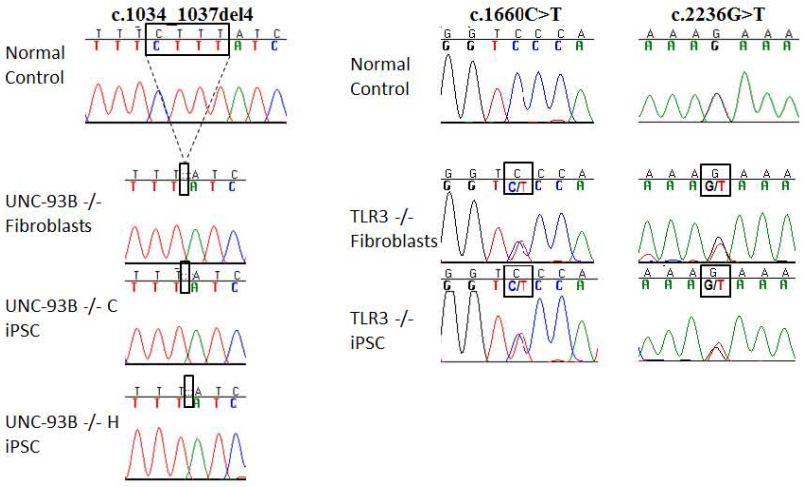
c.1034_1037del4
c.1660C>T
c.2236G>T
Normal Control
Normal Control
UNC-93B -/- Fibroblasts
UNC-93B -/- C iPSC
UNC-93B -/- H iPSC
TLR3 -/- Fibroblasts
TLR3 -/- iPSC

d.

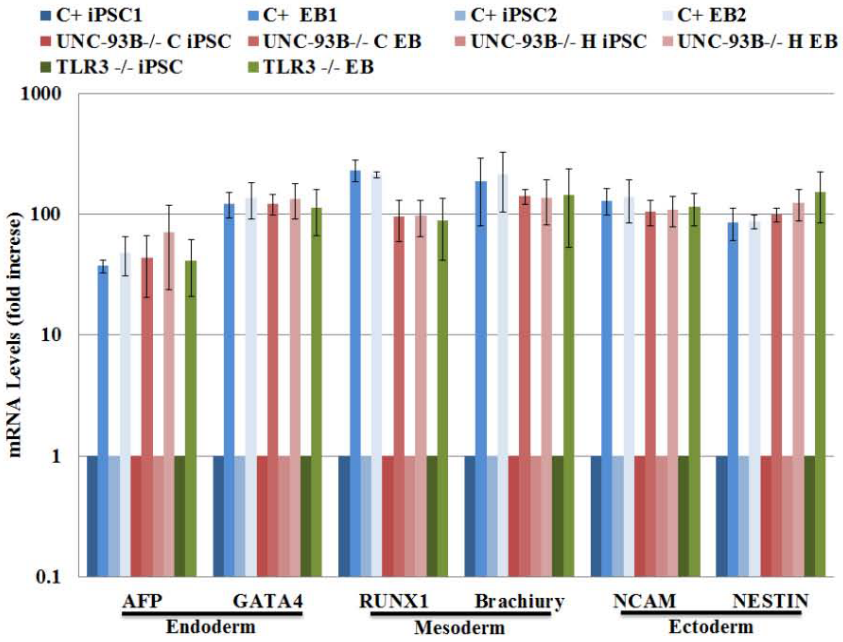
C+ iPSC1
C+ EB1
C+ iPSC2
C+ EB2
UNC-93B-/- C iPSC
UNC-93B-/- C EB
UNC-93B-/- H iPSC
UNC-93B-/- H EB
TLR3 -/- iPSC
TLR3 -/- EB
mRNA Levels (fold increse)
1000
100
10
1
0.1
AFP
GATA4
RUNX1
Brachiury
NCAM
NESTIN
Endoderm
Mesoderm
Ectoderm

Suppl. Figure 1. Characterization of induced pluripotent stem cells (iPSCs) derived from UNC-93B-, TLR3-deficient or healthy control fibroblasts.

a- iPSCs were derived from UNC93B-deficient, TLR3-deficient and control fibroblasts as previously described [13]. The fibroblasts were reprogrammed by transduction with four genes encoding reprogramming factors, *OCT4, SOX2, KLF4,* and *C-MYC,* in a single polycistronic lentiviral vector [14-16]. Cultures were maintained under stringent conditions supporting human embryonic stem cell (hESC) growth [17], and hESC-like colonies emerged five weeks later. Two iPSC lines were expanded and fully characterized for both the healthy control (C^+ iPSC 1 and C^+ iPSC 2) and the UNC-93B-deficient patient ($UNC\text{-}93B^{-/-}$ iPSC line C and $UNC\text{-}93B^{-/-}$ iPSC line H) while one line was derived from the patient with AR complete TLR3 deficiency ($TLR3^{-/-}$). Each of these iPSC lines had a human embryonic stem cell (hESC)-like morphology and expressed pluripotency markers, including SSEA4, TRA-1–81, OCT4, TRA-1-60, SSEA3, and NANOG, as demonstrated by immunofluorescence analysis. Staining with 4,6-diamidino-2-phenylindole (DAPI) was used to determine the total cell content for each image. **b-** The normal, UNC93B-deficient and TLR3-deficient iPSCs had a pluripotency gene expression pattern similar to that seen in previously established control iPSCs. No statistically significant differences in the expression of *OCT4*, *KLF4*, *MYC*, *SOX2*, *NANOG*, *REX1*, *GDF3*, *hTERT*, *RUNX1* and *GATA4* were observed when comparing normal, UNC93B-deficient and TLR3-deficient iPSCs with previously established control iPSCs, as demonstrated by quantitative reverse-transcriptase PCR (qRT-PCR) ($p>0.05$). RT-qPCR results were normalized against those for the β-actin gene. Expression was calculated by the ddCT method, with the results expressed relative to expression levels in the individual parental fibroblast cell lines. Mean values + standard errors (SEM) were calculated from three independent experiments. Statistical analysis was performed by ANOVA test with SHAFFE/Tukey correction for multiple comparisons. In panels **a-** and **b-**, results from two control lines, one TLR3-deficient and two UNC-93B-deficient lines are shown. The data shown are representative of those obtained for the four, three and five lines tested, respectively. **c-** The patient specific iPSCs lines were found to carry the same mutation as the parental fibroblasts. Mutated alleles identical to those in the original specimens were identified by DNA sequencing, confirming the presence of the known *UNC93B1* c.1034_1037del4 mutation, and the known TLR3 c.1660C>T and c.2236G>T mutations, in both the patients' parental fibroblasts and the derived iPSCs. The UNC-93B-deficient and control iPSCs also had an intact karyotype (data not shown). **d-** For confirmation of their pluripotency and multilineage differentiation potential, the iPSCs were allowed to differentiate *in vitro* into embryoid bodies (EB). The EB derived from iPSCs had a typical morphology, similar to that of hESC-derived EB (data not shown) and were equally able to develop into different lineages, as shown by the similar expression levels of markers of all three embryonic germ layers (ectoderm, mesoderm, and endoderm). RT-qPCR gene expression analysis for the derived EB, from control (C+), UNC-93B-deficient ($UNC\text{-}93B^{-/-}$), and the TLR3-deficient ($TLR3^{-/-}$) iPSCs, after 10 days, showed an increase in the expression of lineage markers for the three embryonic germ layers, including: *AFP* and *GATA4* (endoderm), *Brachyury* and *RUNX1* (mesoderm), and *NESTIN* and *NCAM* (ectoderm). Mean values $\pm$ SEM were calculated from three independent experiments.

Suppl. Figure 2

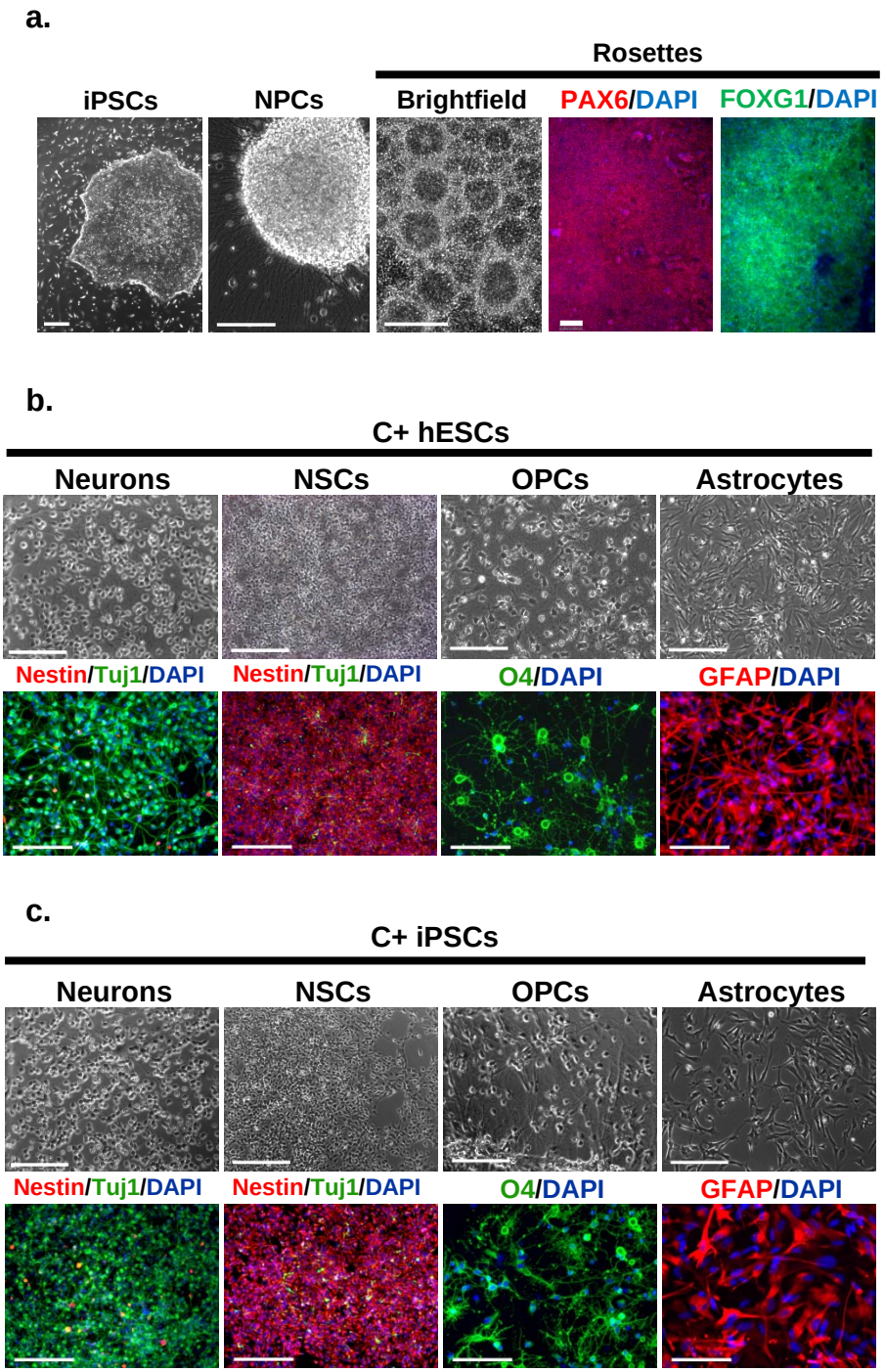

Suppl. Figure 2. Characterization of CNS cell types derived from hESCs and iPSCs

a- Representative phase-contrast images showing the morphology of the TLR3-deficient iPSCs, neural rosettes and NPC clusters as well as immunofluorescence characterization of the rosettes cells for the forebrain marker FOXG1 and for the neuro-ectodermal marker PAX6. **b-, c-** Characterization of control hESC (**b-**)- and control iPSC (**c-**)-derived CNS cell types: Upper panels: phase-contrast images illustrating the characteristic morphologies of each neural cell type; Lower panels: Immunofluorescence analysis for markers of neural stem cells (nestin), neurons (Tuj1), oligodendrocyte progenitor cells (OPCs) (O4) and astrocytes (GFAP). Scale bars in **a-** and **b-** correspond to 100 μm; those in **c-** correspond to 50 μm, except for NSCs (100 μm).

Suppl. Figure 3

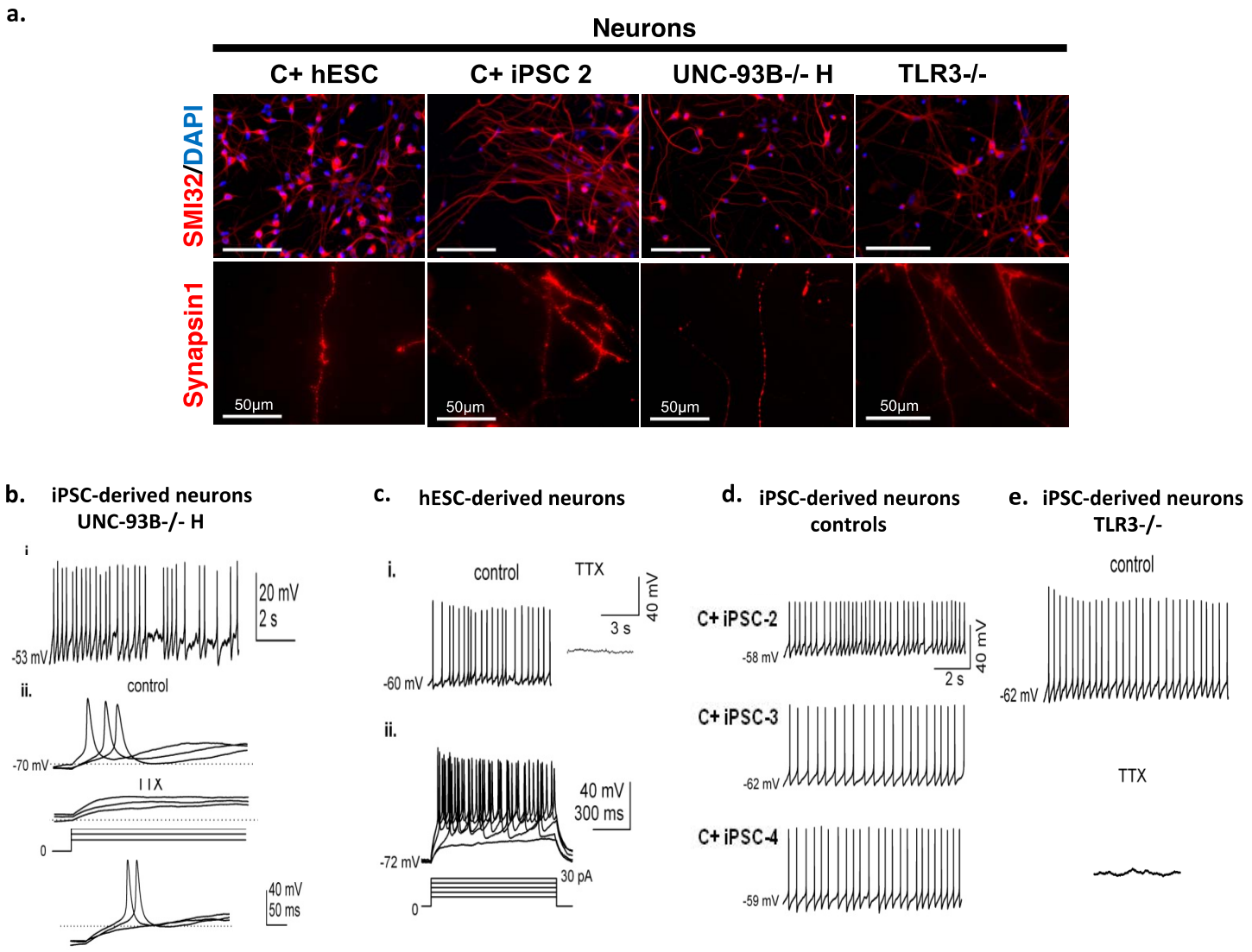

Suppl. Figure 3. Characterization of marker expression and functional properties of neurons derived from disease and control cell lines

a- Immunocytochemical analysis of the expression of a panel of neuronal markers, including SMI-32 and Synapsin-1 in neurons derived from one control hESC (C^+ hESC), one control iPSC (C^+ iPSC), one UNC-93B-deficient iPSC line (UNC-93B$^{-/-}$ H), and one TLR3-deficient iPSC line (TLR3$^{-/-}$). The healthy control iPSC line 'C^+ iPSC 2', and the UNC-93B-deficient iPSC line 'UNC-93B$^{-/-}$ H' were used for differentiation of the neurons used here. **b-** Spontaneous (i) and evoked (ii) action potentials (APs) were observed in two independent UNC-93B-deficient neurons derived from one UNC-93B-deficient iPSC line (UNC-93B$^{-/-}$ H). For evoked APs, the current protocol is shown below (here and in **d-**). Membrane potentials are indicated to the left of each trace here and in subsequent panels. Tetrodotoxin (1 μM) reversibly inhibited spike firing. **c-** Representative voltage traces showing spontaneous (i) and evoked (ii) APs in the same hESC-derived neuron (n = 12: RMP, range -75 to -45 mV, mean: -63.3 ± 3.3 mV, n = 10). Tetrodotoxin (0.5 μM) reversibly inhibited spike firing. **d-** Representative voltage traces of spontaneous AP firing in one neuron derived from each of the indicated control iPSC lines. AP firing was detected in neurons from C^+ iPSC 2 (n = 6: RMP, range, -65 to -58 mV), C^+ iPSC 3 (n = 10: RMP, range, -70 to -59 mV, mean: -64.3 ± 1.4 mV, n = 7) and C^+ iPSC 4 (n = 4: RMP, range -65 to -62 mV, mean: -63.3 ± 0.9 mV, n = 3). In each case, spike firing was inhibited by TTX (0.5 μM; data not shown). **e-** Neurons derived from TLR3-deficient iPSCs were confirmed as such on the basis of their ability to generate Na^+-dependent action potentials (n = 13: RMP, range -72 to -52 mV, mean: -60.3 ± 2.4, n = 9). Membrane potential is indicated to the left of the panel. Representative voltage traces for spontaneous AP firing. Spike firing was inhibited by TTX (0.5 μM).

Suppl. Figure 4

a.

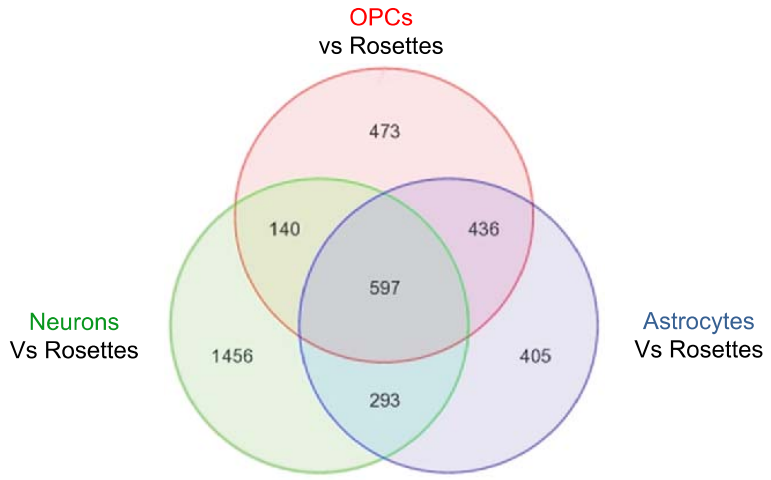

b.

Unbias Top genes only in OPCs

OLIG1	101.5
OLIG2	100.3
APOD	30.5
FAM107A	28.5
NKX6-2	17.3
SCG2	16.7
ANGPTL2	15.9
FAM5C	14.3
S100A16	14.3
FBXO32	13.2
IFIT2	13.1
LRRC38	11.5
NCAM2	11.4
NKX2-2	11.1
PLP1	7.0
SOX10	5.4
PLLP	5.3
MAG	4.0
MBP	2.5

Unbias Top genes only in Astrocytes

A2M	56.9
GFAP	40.5
CD44	29.2
CAPN5	24.5
C1QL1	22.7
SYNM	13.0
HS.204481	10.7
MAN1C1	10.6
IFI16	10.5
GAD1	10.0
PLCH2	10.0
SLC47A2	10.0
RASD1	8.9
CFI	8.8
C21ORF62	8.1
CDKN1A	8.1
SIK1	7.0
HS3ST3A1	6.6
ZNF436	6.3

c.

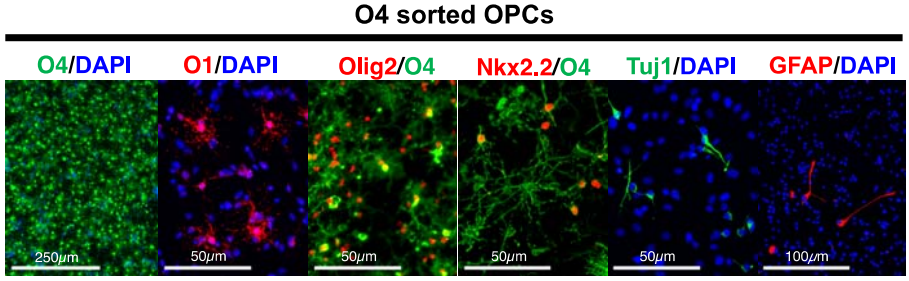

d.

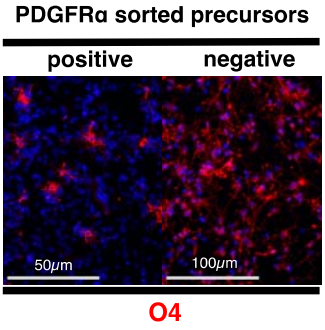

e.

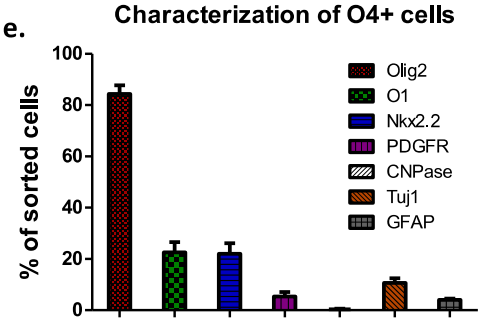

Suppl. Figure 4. Characterization of astrocyte and OPC lineage populations

a- Venn diagram showing a comparison of the genes differentially expressed in microarray analysis of gene expression. RNA was extracted with Trizol reagent (Invitrogen) from purified hESC-derived astrocytes, OPCs, neurons and rosettes, processed by the MSKCC Genomic core facility and hybridized with Illumina human HT-12 oligonucleotide arrays. Gene expression analysis was performed with the Partek Genomics Suite: after quantile normalization, differentially expressed genes were defined for each population (neurons, astrocytes and OPCs, as compared to purified rosettes (p-value ≤ 0.05)). **b-** List of the top 14 genes (upper panel) showing the greatest degree of enrichment and selective expression in OPCs compared to neural rosettes (of 473 genes considered; see **a-**). Additional selected genes for which enrichment was detected in oligodendrocyte progenitor cells (OPCs) are shown below. And list of the top 19 genes (lower panel) with the highest degree of enrichment and displaying selective expression in astrocytes compared to neural rosettes (of 405 genes considered; see **a-**). **c-** Immunocytochemical analysis of the expression of oligodendrocyte lineage markers O4, O1, Olig2 and Nkx2.2, and of markers of neurons (TUJ1) and astrocytes (GFAP) in O4-sorted OPC cultures (three months of differentiation from the hESC stage). **d-** Quantification of marker co-expression in the $O4^+$ cells used in this study. **e-** Immunocytochemical analysis of three-month-old cells two days after PDGFRα sorting. $PDGFR^+$ cell populations contained fewer $O4^+$ OPCs than PDGFR-negative cells.

Suppl. Figure 5

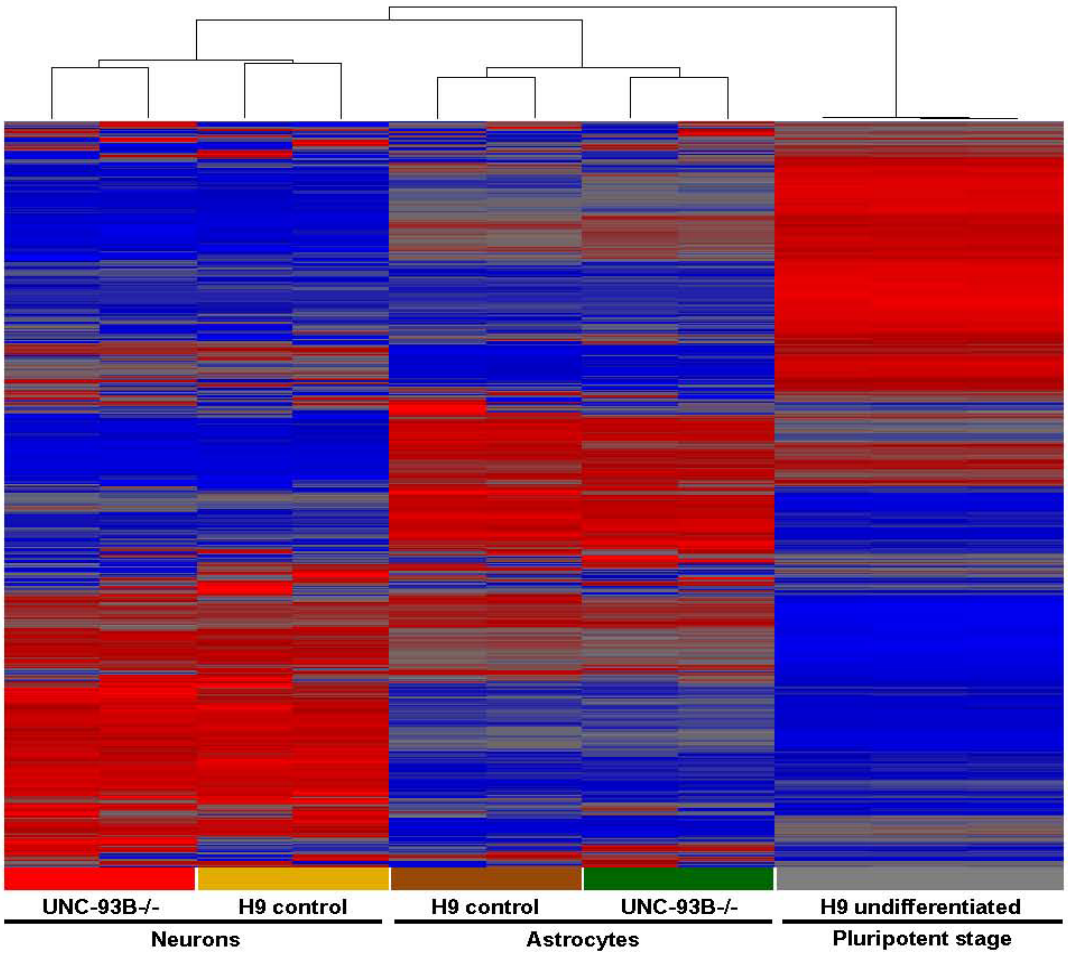

Suppl. Figure 5. UNC-93Bdeficiency does not affect global gene expression profile in neurons and astrocytes, as shown by comparison with control cells differentiated from hESCs

Clustering based on all the genes displaying significant differential expression with respect to hESCs. The gene expression profile in astrocytes and neurons differentiated from UNC-93B-deficient iPSCs line C (UNC-93B$^{-/-}$) or control hESCs line H9 (H9) and that of control hESCs are shown. UNC-93B-deficiency did not significantly alter the overall pattern of gene expression in neurons and astrocytes derived from UNC-93B-deficient iPSCs, as shown by comparison with hESC-derived cells. Results for biological duplicates (for neurons and astrocytes) or triplicates (for undifferentiated H9 hESCs) are shown.

Suppl. Figure 6

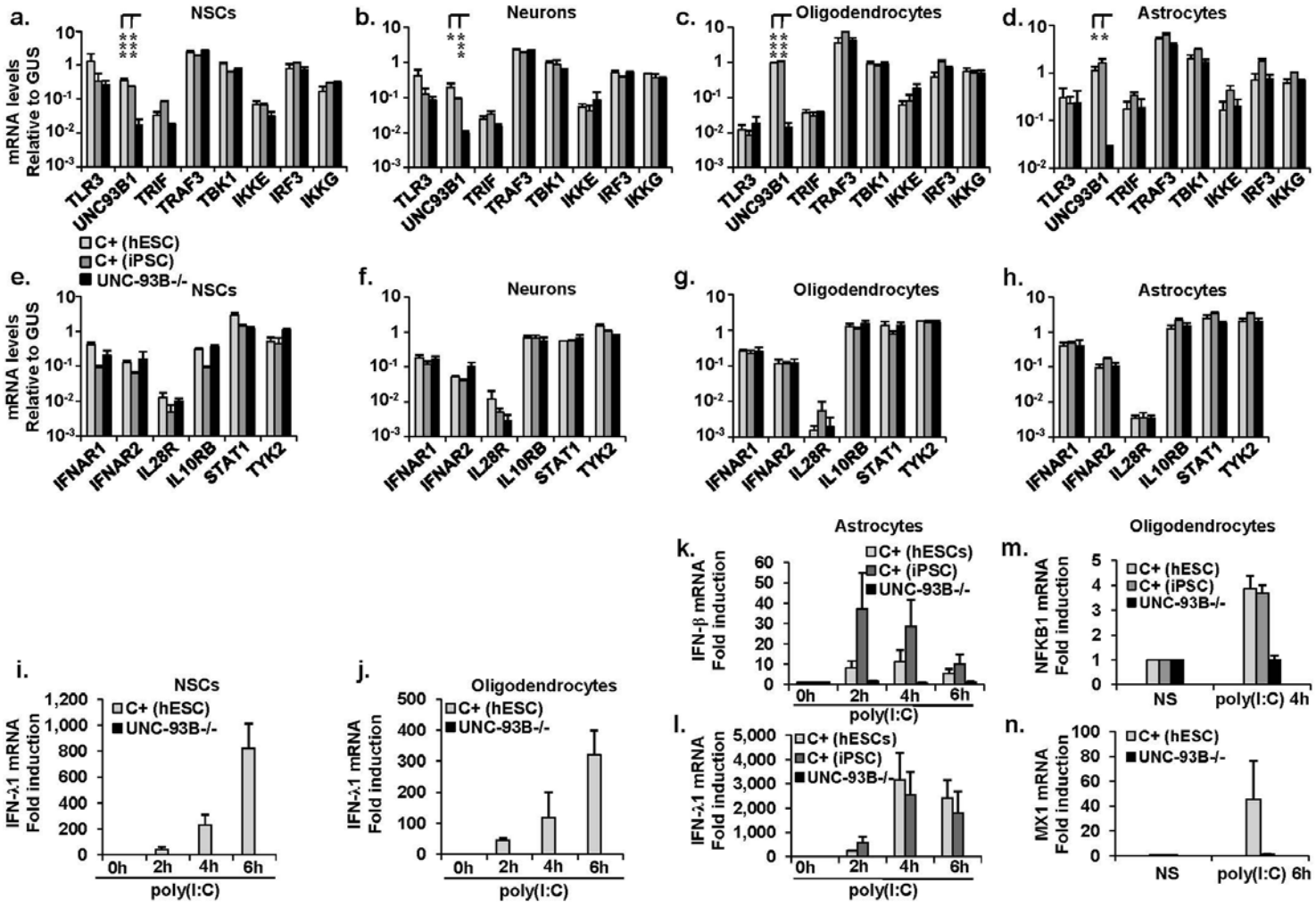

Suppl. Figure 6. UNC-93B-dependent IFN responses to TLR3 in neurons and glial cells

a- to **h-** mRNA levels for TLR3 (**a-** to **d-**) and IFN (**e-** to **h-**) pathway genes, in neural stem cells (NSCs) (**a-**, **e-**), neurons (**b-**, **f-**), oligodendrocytes (**c-**, **g-**) and astrocytes (**d-**, **h-**) differentiated from hESCs from a healthy control (C^+ (hESC), light gray columns), from iPSCs from a healthy control (C^+ (iPSCs),dark gray columns), and from a UNC-93B-deficient patient (UNC-$93B^{-/-}$). Mean values $\pm$ SEM were calculated from two independent experiments, each carried out in duplicate. ANOVA was performed for data shown in **a-** to **h-**. When significant, Dunnett *t* tests were performed for 2X2 comparisons, and significant results are indicated in corresponding panels (* $p<0.05$, *** $p<0.001$). **i-** IFN-λ1 mRNA induction, after 2, 4 or 6 hours of poly(I:C) stimulation, in NSCs differentiated from UNC-93B-deficient iPSCs (UNC-$93B^{-/-}$) or from hESCs from a healthy control (C^+(hESC)). **j-** IFN-λ1 mRNA induction, after 2, 4 or 6 hours of stimulation with poly(I:C), in oligodendrocytes differentiated from UNC-93B-deficient iPSCs (UNC-$93B^{-/-}$), or from hESCs from a healthy control (C^+(hESC)). **k- and l-** IFN-β (**k-**) or IFN-λ1 (**l-**) mRNA induction, after 2, 4 or 6 hours of stimulation with poly(I:C), in astrocytes differentiated from UNC-93B-deficient iPSCs (UNC-$93B^{-/-}$), from iPSCs from two healthy controls, or from hESCs from a healthy control (C^+(hESC)). **m-** NFKB1 mRNA induction, after 4 hours of stimulation with poly(I:C), in oligodendrocytes differentiated from UNC-93B-deficient iPSCs (UNC-$93B^{-/-}$), from hESCs from a healthy control (C^+(hESC)), or from iPSCs from a healthy control (C^+ (iPSC)). **n-** MX1 mRNA induction, after 6 hours of stimulation with poly(I:C), in oligodendrocytes differentiated from UNC-93B-deficient iPSCs (UNC-$93B^{-/-}$), or from hESCs from a healthy control (C^+(hESC)). For the data shown in **i-** to **n-**, mean values $\pm$ SEM were calculated from two independent experiments, each carried out in duplicate. Student's *t* tests showed a significant induction of IFN-β, IFN-λ1, NFKB1 or MX1 in all cells from all the controls tested ($p<0.05$), but not in UNC-93B-deficient cells. One healthy control line 'C^+ iPSC 3' was used in **a-**, **d-**, **e-** and **h-**. One healthy control line (C^+ iPSC 2) is used in **b-**, **d-**, **f-**, **g-** and **m-**. Two healthy controls lines (C^+iPSC 3 and C^+ iPSC 4) were used in **k- and l-**. Mean values $\pm$ SEM calculated from the two iPSC controls are presented. The UNC-93B-deficient iPSC line 'UNC-$93B^{-/-}$ C' was used in experiments **a-** through **n-**.

Suppl. Figure 7

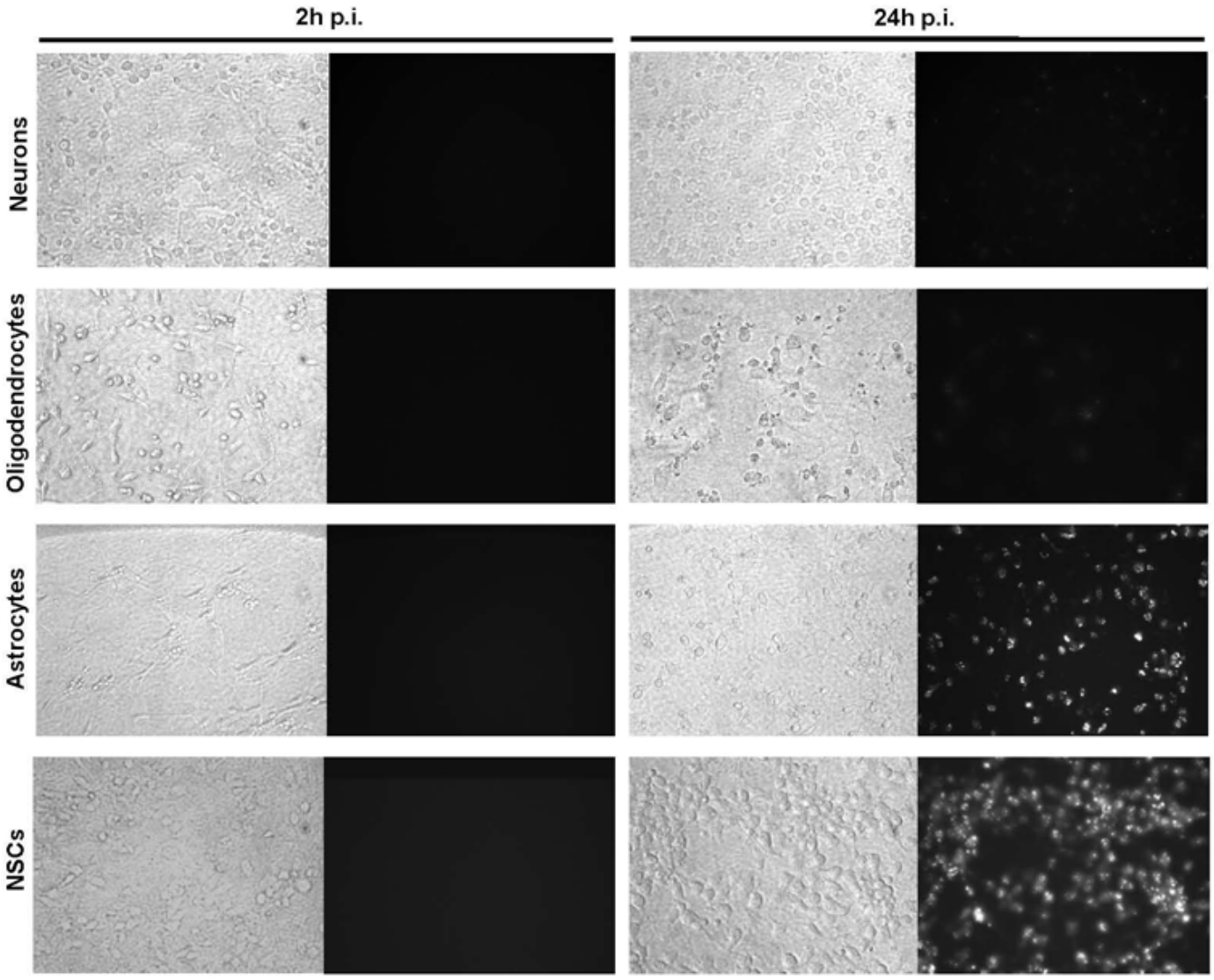

Suppl. Figure 7. HSV-1-GFP infection in central nervous system cells

Representative images showing GFP expression in HSV-1-GFP infected healthy control central nervous system (CNS) cells. After 2 or 24 hours of infection with HSV-1-GFP at a MOI of 1, GFP expression in neurons, oligodendrocytes, astrocytes and NSCs differentiated from hESCs from a healthy control was visualized under a fluorescence microscope and shown. Phase-contrast photomicrographs of the NSCs, neurons, oligodendrocytes and astrocytes from the same field are also shown.

Suppl. Figure 8

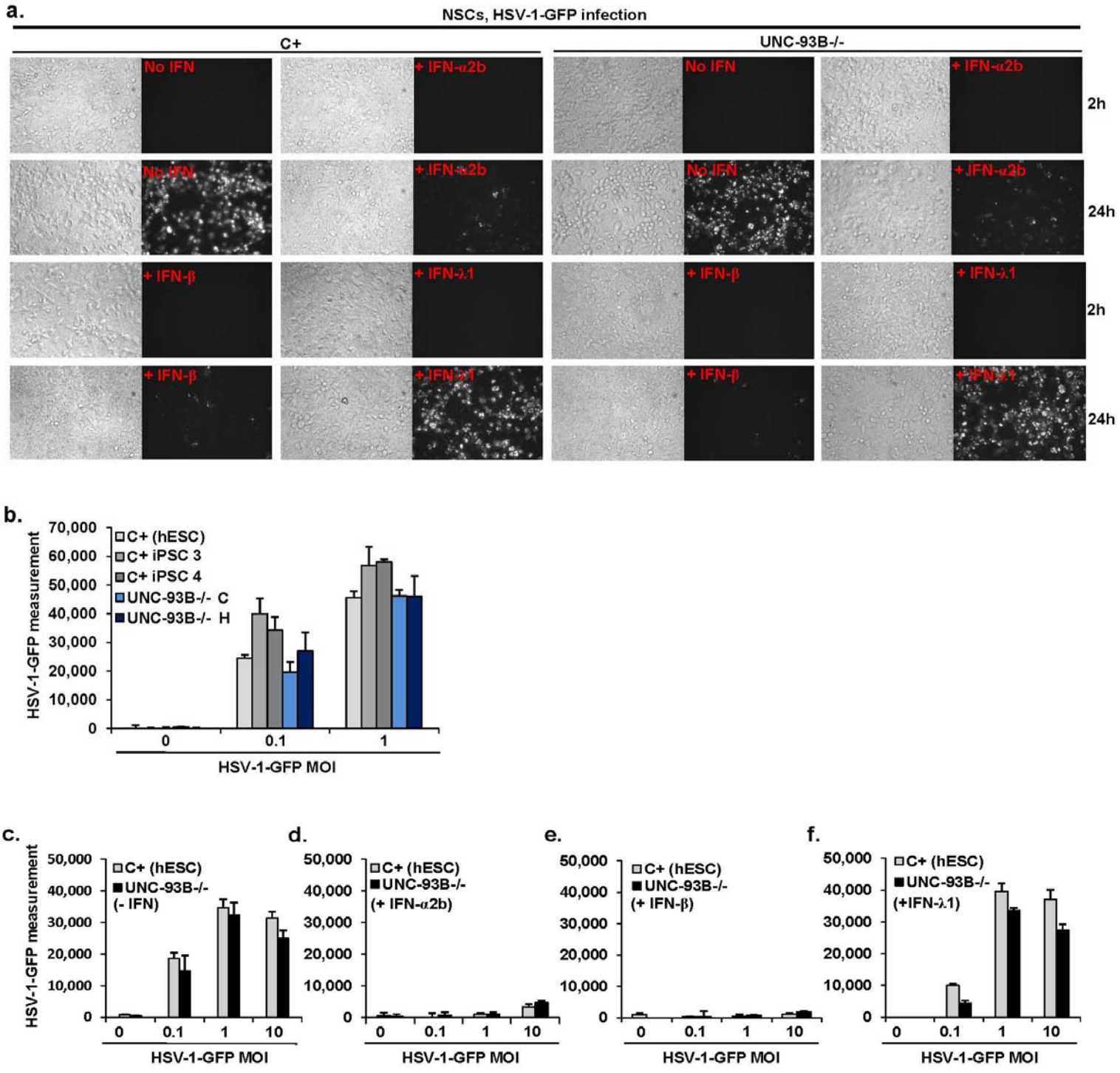

Suppl. Figure 8. HSV-1-GFP infection in UNC-93B-deficient and control NSCs

a- Representative images showing GFP expression in HSV-1-GFP infected NSCs from healthy controls or UNC-93B-deficient patient. After 2 and 24 hours of infection with HSV-1-GFP at a MOI of 1, GFP expression in NSCs differentiated from hESCs from a healthy control (C^+) (left panel) or from UNC-93B-deficient (UNC-93B$^{-/-}$) iPSCs (right panel), with or without IFN-α2b, IFN-β or IFN-λ1 treatment, was visualized by fluorescence microcopy. Phase-contrast photomicrographs of the NSCs from the same field are also shown. The UNC-93B-deficient iPSC line 'UNC-93B$^{-/-}$ C' was used here for NSC differentiation for this experiment. **b-** After 24 hours of infection with various MOI of HSV-1-GFP, the GFP expression in NSCs differentiated from two lines of UNC-93B-deficient iPSCs (UNC-93B$^{-/-}$ C, UNC-93B$^{-/-}$ H), from iPSCs from two healthy controls, one line each (C^+ iPSC 3, C^+ iPSC 4), or from hESCs from a healthy control (C^+ (hESC)),without IFN treatment, was assessed with a fluorescence plate reader. The difference in GFP fluorescence intensity between HSV-1-GFP-infected cells and uninfected cells is shown. ANOVA and subsequent Dunnett *t* tests showed that GFP levels in UNC-93B-deficient NSCs were not significantly higher than those of the healthy controls tested. **c-, d-, e-, f-** After 24 hours of infection with various MOI of HSV-1-GFP, the GFP expression in NSCs differentiated from UNC-93B-deficient iPSCs, or from hESCs from a healthy control, without IFN treatment (**c-**) or upon treatment with IFN-α2b (**d-**), IFN-β (**e-**) or IFN-λ1 (**f-**), was assessed with a fluorescence plate reader. The difference in GFP fluorescence intensity between HSV-1-GFP-infected cells and uninfected cells is shown. In **c-** to **f-**, the UNC-93B-deficient iPSC line 'UNC-93B$^{-/-}$C' was used for NSC differentiation. For the data shown in **b-**, mean values $\pm$ SEM were calculated from a single experiment, carried out in triplicate. For the data shown in **c-, d-, e-** and **f-**, mean values $\pm$ SEM were calculated from two independent experiments, each carried out in triplicate.

Suppl. Figure 9

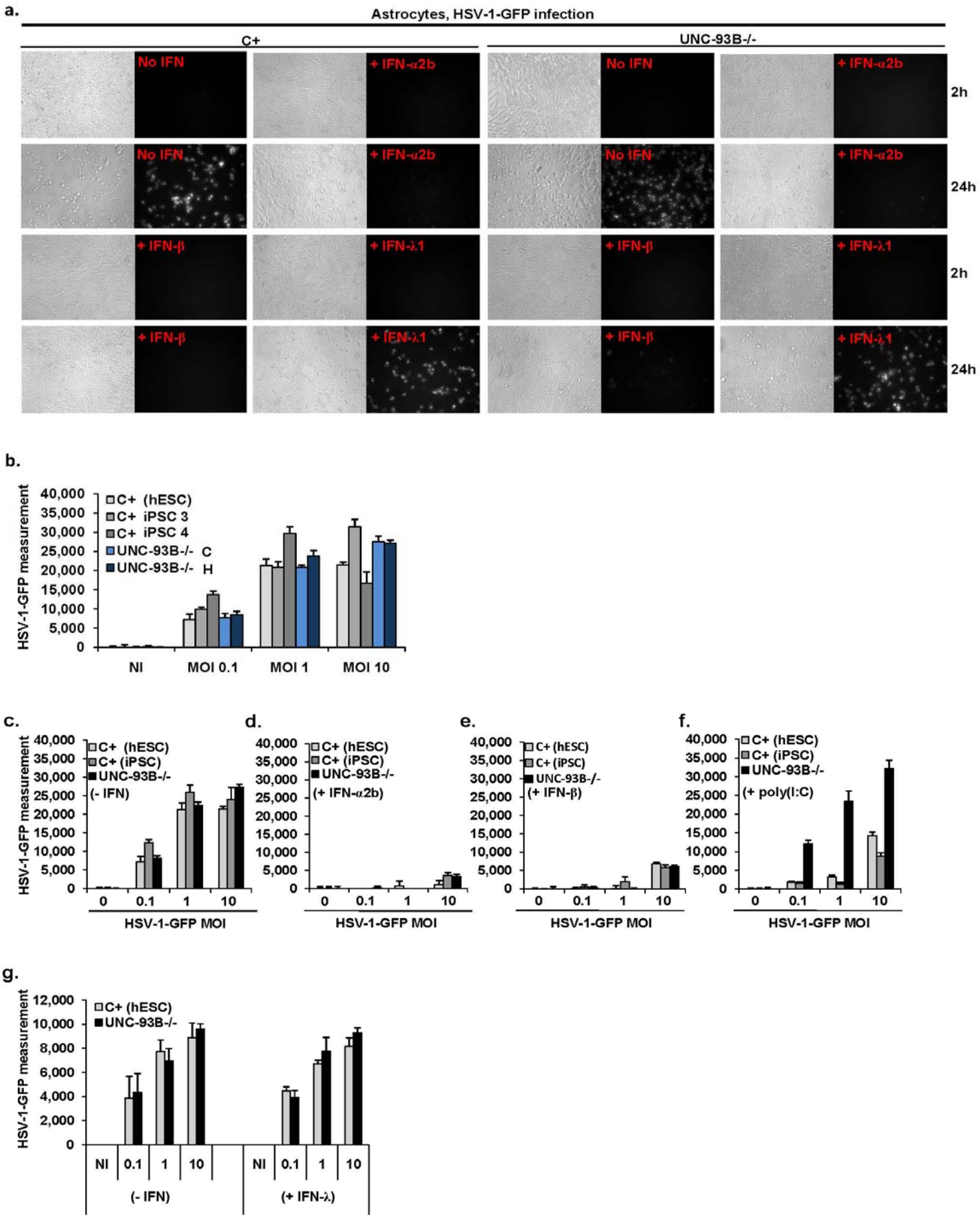

Suppl. Figure 9. HSV-1-GFP infection in UNC-93B-deficient and control astrocytes

a- Representative images showing GFP expression in HSV-1-GFP infected astrocytes from healthy controls or UNC-93B-deficient patient. After 2 and 24 hours of infection with HSV-1-GFP at a MOI of 1, GFP expression in astrocytes differentiated from hESCs from a healthy control (C^+) (left panel) or from UNC-93B-deficient iPSCs (UNC-93B$^{-/-}$) (right panel), with or without IFN-α2b, IFN-β or IFN-λ1 treatment, was visualized by fluorescence microcopy. Phase-contrast photomicrographs of the astrocytes from the same field are also shown. The UNC-93B-deficient iPSC line 'UNC-93B$^{-/-}$ C' was used for the differentiation of astrocytes for this experiment. **b-** After 24 hours of infection with various MOI of HSV-1-GFP, GFP expression in astrocytes differentiated from two lines of UNC-93B-deficient iPSCs (UNC-93B$^{-/-}$ C, UNC-93B$^{-/-}$ H), iPSCs from two healthy controls, one line each (C^+ iPSC 3), C^+ iPSC 4)), or from hESCs from a healthy control (C^+ (hESC)), without IFN treatment, was assessed with a fluorescence plate reader. The difference in GFP fluorescence intensity between HSV-1-GFP-infected cells and uninfected cells is shown. ANOVA and subsequent Dunnett *t* tests showed GFP levels in UNC-93B-deficient astrocytes were not significantly higher than those of the healthy controls tested. **c-, d-, e-** and **f-** After 24 hours of infection with various MOI of HSV-1-GFP, GFP expression in astrocytes differentiated from UNC-93B-deficient iPSCs (UNC-93B$^{-/-}$), from iPSCs from two healthy controls, one line each (C^+ iPSC 3, C^+ iPSC 4), or from hESCs from a healthy control (C^+ (hESC)) ,without any treatment (**c-**), or upon treatment with IFN-α2b (**d-**), IFN-β (**e-**) or poly(I:C) (**f-**), was measured with a fluorescence plate reader. The difference in GFP fluorescence intensity between HSV-1-GFP-infected cells and uninfected cells is shown. **g-** After 24 hours of infection with various MOI of HSV-1-GFP, GFP expression in astrocytes differentiated from UNC-93B-deficient iPSCs, or from hESCs from a healthy control, without IFN treatment (left panel), or upon treatment with IFN-λ1 (right panel), was measured with a fluorescence plate reader. The difference in GFP fluorescence intensity between HSV-1-GFP-infected cells and uninfected cells is shown. In **c-** to **g-**, the UNC-93B-deficient iPSC line 'UNC-93B$^{-/-}$ C' was used for the differentiation of astrocytes. For the data shown in **b-** to **g-**, mean values $\pm$ SEM were calculated from two independent experiments, each carried out in triplicate.

Suppl. Figure 10

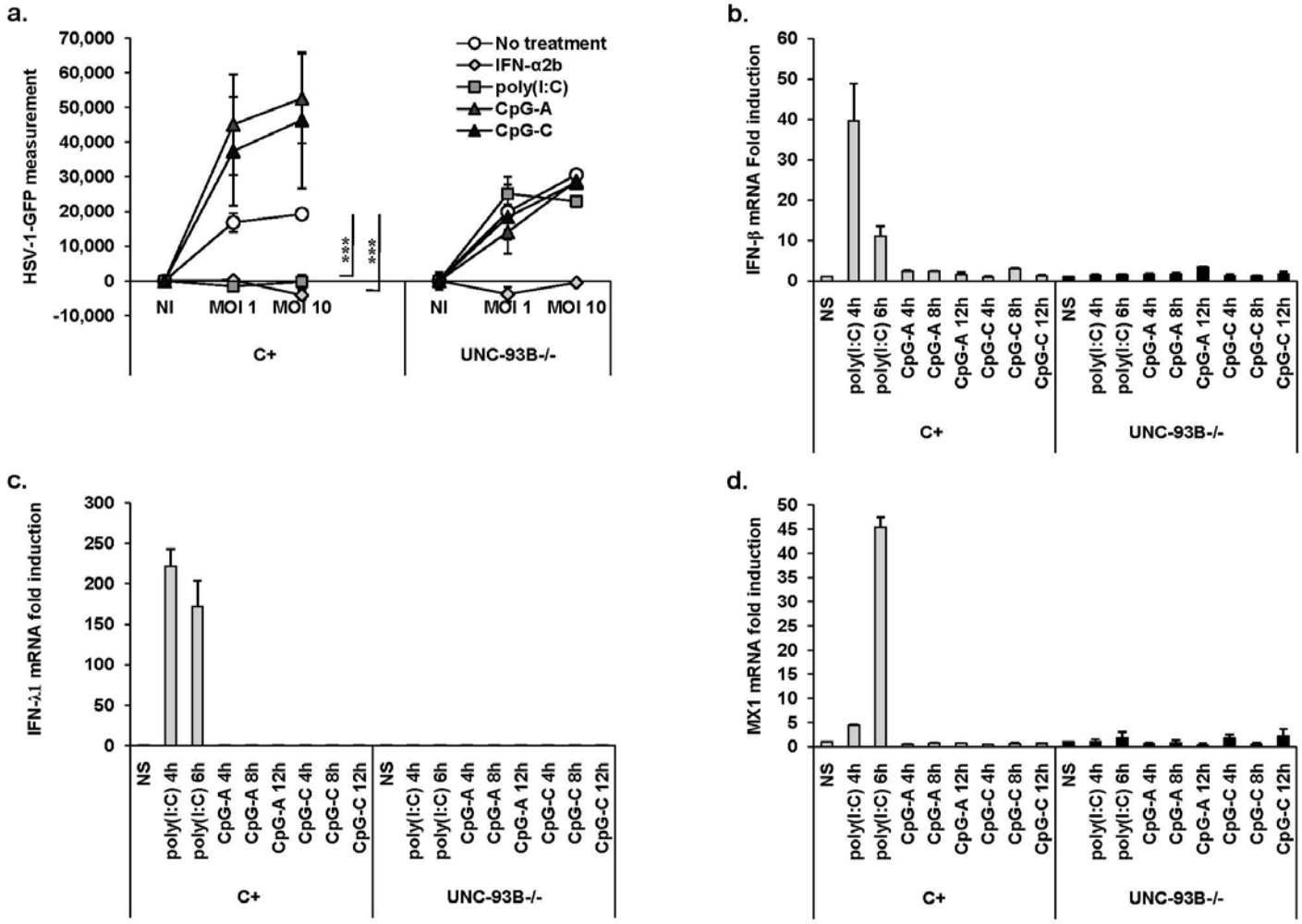

Suppl. Figure 10. Protective effect of poly(I:C) treatment against HSV-1-GFP infection in control but not UNC-93B-deficient astrocytes

a- After 24 hours of infection with various MOI of HSV-1-GFP, GFP expression in astrocytes differentiated from UNC-93B-deficient iPSCs (UNC-93B$^{-/-}$) or from hESCs from a healthy control (C^{+}), without IFN treatment, treated with IFN-α2b, poly(I:C), CpG-A or CpG-C, was measured with a fluorescence plate reader. The difference in GFP fluorescence intensity between HSV-1-GFP-infected cells and uninfected cells is shown. Mean values ± SEM were calculated from two independent experiments, each carried out in triplicate. ANOVA was performed for data shown in **a-,** from UNC-93B$^{-/-}$ or from C^{+} astrocytes, without IFN treatment, treated with IFN-α2b or poly(I:C). When significant, Dunnett *t* tests were performed for 2X2 comparisons, and significant results are indicated in corresponding panels (*** $p<0.001$). **b-, c-** and **d-** IFN-β (**b-**), IFN-λ1 (**c-**) or MX1 (**d-**) mRNA induction, after 4 or 6 hours of poly(I:C) stimulation, or 4, 8 or 12 hours of CpG-A or CpG-C stimulation, in astrocytes differentiated from UNC-93B-deficient iPSCs (UNC-93B$^{-/-}$) or from hESCs from a healthy control (C^{+}). Mean values ± SEM were calculated from two independent experiments, each carried out in duplicate. In **a-** to **d-**, the UNC-93B-deficient iPSC line 'UNC-93B$^{-/-}$C' was used for the differentiation of astrocytes. Student's *t* tests showed that IFN-β, IFN-λ1 and MX1 were all significantly induced after poly(I:C) stimulations, in the C^{+} cells tested ($p<0.001$), but not in UNC-93B-deficient cells.

Suppl. Figure 11

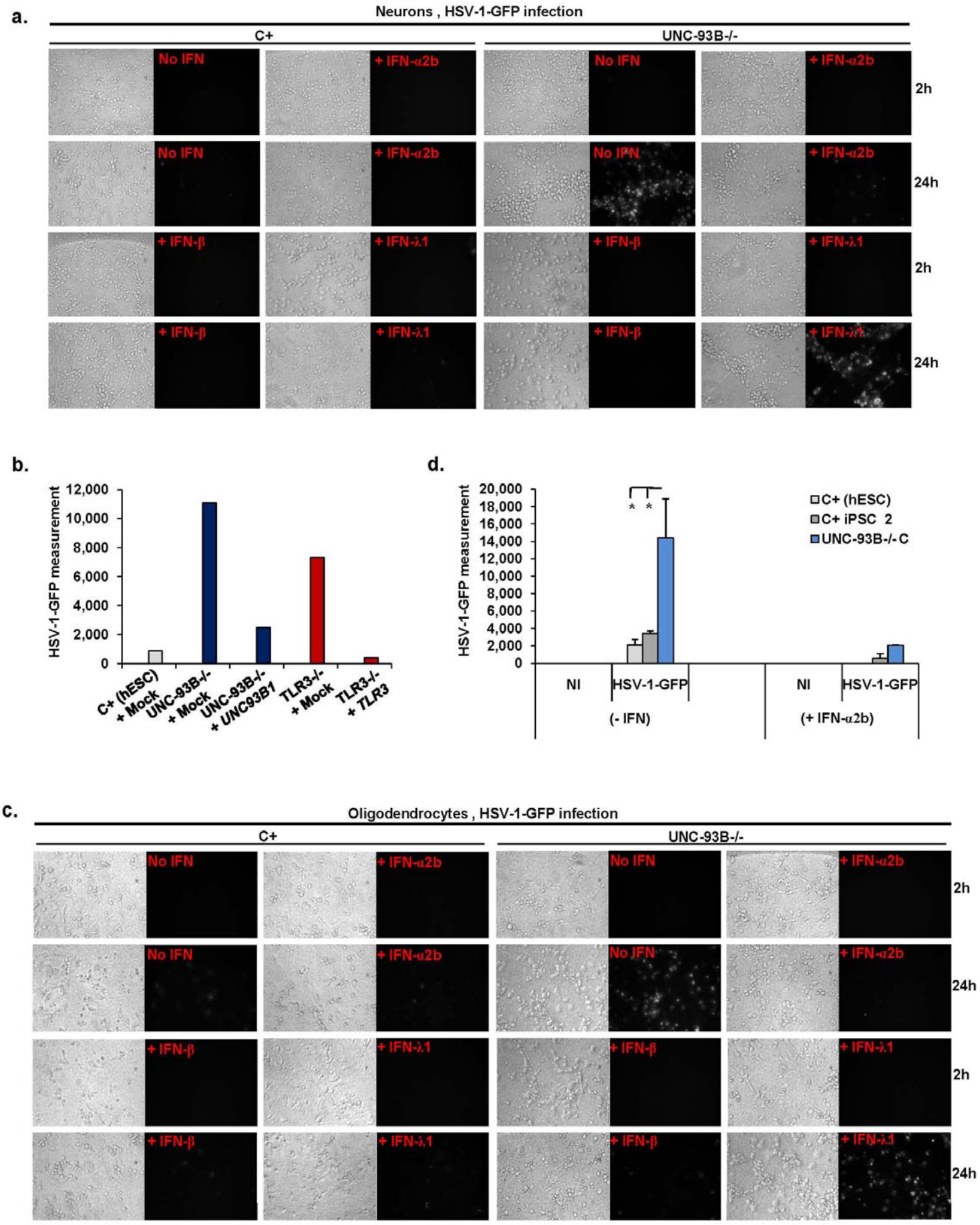

Suppl. Figure 11. UNC-93B- or TLR3-deficient neurons and oligodendrocytes are susceptible to HSV-1 infection

a- Representative images showing GFP expression in HSV-1-GFP infected neurons from healthy controls or UNC-93B-deficient patient. After 2 and 24 hours of infection with HSV-1-GFP at a MOI of 1, GFP expression in neurons differentiated from hESCs from a healthy control (C^+) (left panel), from UNC-93B-deficient iPSCs ($UNC\text{-}93B^{-/-}$) (right panel), with or without IFN-α2b, IFN-β or IFN-λ1 treatment was visualized by fluorescence microcopy. Phase-contrast photomicrographs of the neurons from the same field are also shown. The UNC-93B-deficient iPSC line 'UNC-$93B^{-/-}$ C' was used for the differentiation of neurons for this experiment. **b-** After 2 and 24 hours of infection with HSV-1-GFP at a MOI of 1, GFP expression was assessed with a fluorescence plate reader, in UNC-93B-deficient neurons (differentiated from UNC-$93B^{-/-}$ iPSC line H), after infection with a lentivirus containing human WT *UNC93B1* (UNC-$93B^{-/-}$ + *UNC93B1*) or a mock construct (UNC-$93B^{-/-}$ + Mock);in TLR3-deficient neurons, after infection with a lentivirus containing human WT *TLR3* ($TLR3^{-/-}$ + *TLR3*) or a mock construct ($TLR3^{-/-}$ + Mock); and neurons differentiated from one healthy control hESC line, after infection with a lentivirus containing a mock construct (C^+ (hESC) + Mock). The difference in GFP fluorescence intensity between HSV-1-GFP-infected cells and uninfected cells is shown. **c-** Representative images showing GFP expression in HSV-1-GFP infected oligodendrocytes from healthy controls or UNC-93B-deficient patient. After 2 or 24 hours of infection withHSV-1-GFP at a MOI of 1, GFP expression in oligodendrocytes differentiated from hESCs from a healthy control (C^+) (left panel), from UNC-93B-deficient iPSCs ($UNC\text{-}93B^{-/-}$) (right panel), with or without IFN-α2b, IFN-β or IFN-λ1 treatment, was visualized by fluorescence microcopy. Phase-contrast photomicrographs of the oligodendrocytes from the same field are also shown. The UNC-93B-deficient iPSC line 'UNC-$93B^{-/-}$ C' was used for the differentiation of oligodendrocytes. **d-** After 24 hours of infection with HSV-1-GFP at a MOI of 1, GFP expression was measured with a fluorescence plate reader in oligodendrocytes differentiated from UNC-93B-deficient iPSCs line C (UNC-$93B^{-/-}$ C), from hESCs from a healthy control (C^+ hESC) and iPSCs from a healthy control (C^+ iPSC 2), without (left panel) or with (right panel) IFN-α2b treatment. The difference in GFP fluorescence intensity between HSV-1-GFP-infected cells and uninfected cells is shown. Mean values $\pm$ SEM were calculated from two independent experiments, each carried out in duplicate. ANOVA was performed for data shown in **d-**. When significant, Dunnett *t* tests were performed for 2X2 comparisons, and significant results are indicated in corresponding panels (* $p<0.05$).

Suppl. Figure 12

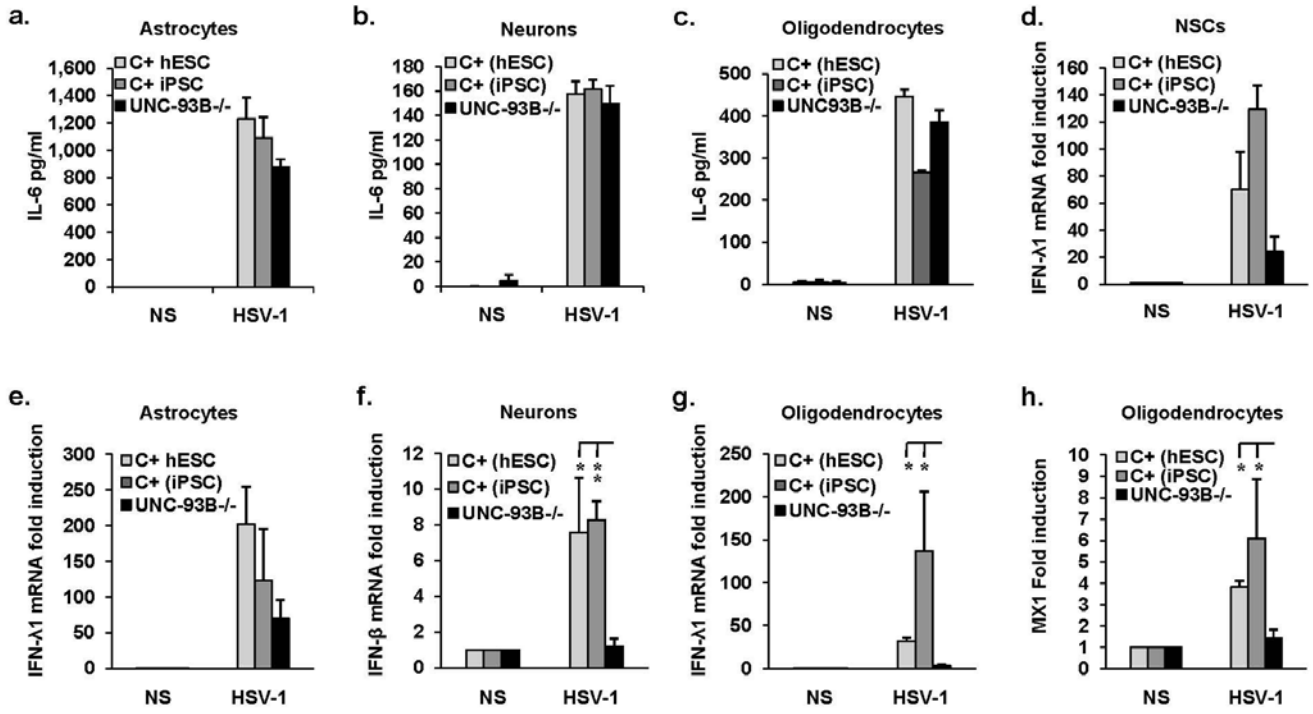

Suppl. Figure 12. Responses to HSV-1 infection in neurons and glial cells

a-, b- and **c-** IL-6 production, as measured by ELISA, in astrocytes (**a-**), neurons (**b-**) and oligodendrocytes (**c-**) differentiated from UNC-93B-deficient iPSCs (UNC-93B$^{-/-}$), hESCs from a healthy control (C^+(hESC)) and iPSCs from a healthy control (C^+(iPSC)), after 24 hours of infection with HSV-1. Mean values $\pm$ SEM were calculated from two independent experiments, each carried out in duplicate. **d-, e-,** IFN-λ1 mRNA induction, as measured by RT-qPCR, after 24 hours of HSV-1 infection, in NSCs (**d-**) and astrocytes (**e-**) differentiated from UNC-93B-deficient iPSCs (UNC-93B$^{-/-}$), hESCs from a healthy control (C^+ hESC), or iPSCs from a healthy control (C^+ iPSC). **f-** IFN-β mRNA induction, as measured by RT-qPCR, after 24 hours of HSV-1 infection, in neurons differentiated from UNC-93B-deficient iPSCs (UNC-93B$^{-/-}$), hESCs from a healthy control (C^+ hESC), or iPSCs from a healthy control (C^+ iPSC). **g-** IFN-λ1 mRNA induction, as measured by RT-qPCR, after 24 hours of HSV-1 infection, in oligodendrocytes differentiated from UNC-93B-deficient iPSCs (UNC-93B$^{-/-}$), hESCs from a healthy control (C^+ hESC), or iPSCs from a healthy control (C^+ iPSC). For the data shown in **d-** to **g-**, mean values $\pm$ SEM were calculated from three independent experiments, each carried out in duplicate. **h-** MX1 mRNA induction, after 24 hours of stimulation with HSV-1, in oligodendrocytes differentiated from UNC-93B-deficient iPSCs line C (UNC-93B$^{-/-}$), from hESCs from a healthy control (C^+ hESC), or from iPSCs from a healthy control (C^+ iPSC). Mean values $\pm$ SEM were calculated from two independent experiments, each carried out in duplicate. In **a-** to **h-**, UNC-93B-deficient iPSC line 'UNC-93B$^{-/-}$C' and one hESC healthy control line were used for the differentiation of various types of CNS cells, the healthy control iPSC line 'C^+ iPSC 2' was used for the differentiation of neurons and oligodendrocytes, the healthy control iPSC line 'C^+ iPSC 3' was used for the differentiation of NSCs and astrocytes. ANOVA was performed for data shown in **a-** to **h-**. When significant, Dunnett *t* tests were performed for 2X2 comparisons, and significant results are indicated in corresponding panels (* $p<0.05$, ** $p<0.01$).

Supple. Table 1. Table of experiments on CNS cells, iPSC and hESC lines, and figures

Experiment	No. of UNC-93B$^{-/-}$ lines	No. of control lines	No. of TLR3$^{-/-}$ lines	Figures
Generation and characterization of iPSCs	5 (2 characterized)	4(2 newly characterized and 2 previously described)	2 (1 characterized)	1A-B, S1A-D
Differentiation to NPC, NSCs, neurons, oligocytes, astrocytes.	2 (lines H and C)	iPSC-1, 2, 3, 4 and hESC H9	Line L	2, S2A-D
Action potential of iPSC-derived neurons	line H	iPSC 2, 3, 4 and hESC H9	Line L	S3B-C-E
Gene expression profile in iPSC-derived glial cells	line C	hESC H9		S4, Table S4
Fine characterization of glial cells	line C	iPSC 2 and hESC H9		S2C-D
Expression of genes of the TLR3 pathway	line C	iPSC 2, 3 and hESC H9		S7A-H
Induction of IFN and IFN-target genes by poly(I:C)	line C	iPSC 2, 3, 4 and hESC H9		3, S7I-N
Rescue of poly(I:C)-induced expression of IFN	line C	iPSC 2 and hESC H9		3B-D,
HSV1-GFP replication in control hESC-derived CNS cells		hESC H9		S9
HSV1-GFP replication in iPSC-derived NSC and astrocytes	line C and H	iPSC 3, 4 and hESC H9		4A-C, S10, S11
Rescue of HSV-1-GFP replication with IFN-α2b or IFN-β in NSCs and astrocytes	line C	iPSC 3, 4 and hESC H9		S10A, S10C-E, S11A, S11C-E,
Rescue of HSV-1-GFP replication in control, but not in UNC93B$^{-/-}$ astrocytes, with poly(I:C)	line C	iPSC 3,4 and hESC H9		S11F
No rescue of HSV-1-GFP replication with IFN-λ1 in NSCs and astrocytes	line C	hESC H9		S10F, S11G
CpG fails to reduce HSV-1 replication in astrocytes	line C	hESC H9		S12A-D
HSV-1-GFP replication in neurons	lines C and H	iPSC 1, 2, 3, 4 and hESC H9	line L	4A, 4D, 4E, S13A-B
Rescue of HSV-1-GFP replication in neurons by IFN α2b or IFN-β but not by IFN-λ1	line C	hESC H9		S13A

Rescue of HSV-1-GFP replication in neurons by gene rescue	line H	iPSC 2 and hESC H9	line L	4F, S13B
HSV-1-GFP replication in oligodendrocytes	line C	iPSC 2 and hESC H9		4A, 4G, S14A-B
Rescue of HSV-1-GFP replication in oligodendrocytes by IFN α2b or IFN-β but not by IFN-λ1	line C	iPSC 2 and hESC H9		S14A-B
Production of IFNs and inflammatory cytokines after HSV-1 infection	line C	iPSC 2,3,4 and hESC H9		4H-K, S15

Note:

Control iPSC line 1 = R2CFii = C^+ iPSC 1

Control iPSC line 2 = R2CFiv =C^+ iPSC 2

Control iPSC line 3 = SeV6 = C^+ iPSC 3 (ref [21])

Control iPSC line 4 = C14 = C^+ iPSC 4 (ref [22])

<u>Suppl. Table 2.</u> Total number of variants revealed by whole-exome sequencing in iPSC lines and their parental fibroblast lines

	Cell line	Total number of variant	Intersection	Concordance
Comparison 1	Control fibroblasts	72829	68391	99.94790581
	Control iPSCs	83671		
Comparison 2	UNC-93B$^{-/-}$ fibroblasts	68905	64924	99.95158444
	UNC-93B$^{-/-}$ iPSC line C	67382		
Comparison 3	UNC-93B$^{-/-}$ fibroblasts	68905	65463	99.9550708
	UNC-93B$^{-/-}$ iPSC line H	69520		
Comparison 4	UNC-93B$^{-/-}$ iPSC line C	67382	64788	99.9545369
	UNC-93B$^{-/-}$iPSC line H	69520		
Comparison 5	TLR3$^{-/-}$ fibroblasts	72264	66442	99.96039725
	TLR3$^{-/-}$ iPSCs	71184		

Note:

* Total number of variant = total number of single nucleotide variations and indels.

* Intersection = number of variant calls common to the two call sets being compared.

* Concordance = percent genotype concordance of the intersection call set.

* Differences between the number of variants and concordance were checked by manual inspection of the alignments and result from:

1. Ambiguous alignments in repeat-rich and duplicated regions, leading to false positive variant calls.

2. Technical limitations in indel calling resulting in a higher error rate than for single-nucleotide variant calls.

3. Insufficient read coverage to make confident genotype calls

Suppl. Table 3. List of genes carrying non reported exonic variants revealed by whole-exome sequencing in control or patient iPSC lines, or their parental fibroblasts. Only variants not common to iPSC lines and their respective parental fibroblasts are taken into account here.

Control iPSCs

No.	Chr	Gene name	Transcript ID	Effect	Hom/Het
1	1	MIB2	ENST00000520777	Nonsynonymous	Het
2	1	FHAD1	ENST00000375999	Stop gained	Het
3	1	SLC9A1	ENST00000545949	Synonymous	Het
4	1	FAM167B	ENST00000373582	Nonsynonymous	Het
5	1	SYDE2	ENST00000341460	Synonymous	Het
6	1	TNR	ENST00000367674	Synonymous	Het
7	1	CRB1	ENST00000543483	Nonsynonymous	Het
8	2	GREB1	ENST00000381486	Synonymous	Het
9	2	ARHGAP25	ENST00000497079	Nonsynonymous	Het
10	2	SP3	ENST00000455789	Nonsynonymous	Het
11	2	C2orf85	ENST00000343216	Synonymous	Het
12	3	VILL	ENST00000383759	Nonsynonymous	Het
13	3	CELSR3	ENST00000544264	Synonymous	Het
14	3	MSL2	ENST00000434835	Synonymous	Het
15	3	MSL2	ENST00000434835	Nonsynonymous	Het
16	3	SOX2	ENST00000431565	Synonymous	Het
17	4	CXXC4	ENST00000426831	Synonymous	Het
18	5	NR2F1	ENST00000327111	Synonymous	Het
19	5	YTHDC2	ENST00000511372	Nonsynonymous	Het
20	5	LRRTM2	ENST00000274711	Synonymous	Het
21	5	LRRTM2	ENST00000274711	Nonsynonymous	Het
22	5	PCDHGB4	ENST00000519479	Nonsynonymous	Het

23	6	BRD2	ENST00000449085	Nonsynonymous	Het
24	6	PNPLA1	ENST00000457797	Synonymous	Het
25	7	RADIL	ENST00000538469	Nonsynonymous	Het
26	7	NEUROD6	ENST00000297142	Synonymous	Het
27	7	BMPER	ENST00000436222	Nonsynonymous	Het
28	7	LHFPL3	ENST00000543266	Synonymous	Het
29	7	CCDC136	ENST00000464832	Nonsynonymous	Het
30	8	RP1L1	ENST00000382483	Synonymous	Het
31	8	KAT6A	ENST00000406337	Nonsynonymous	Het
32	8	PLAG1	ENST00000429357	Nonsynonymous	Het
33	8	C8orf45	ENST00000541540	Nonsynonymous	Het
34	9	BNC2	ENST00000380666	Nonsynonymous	Het
35	9	BNC2	ENST00000484726	Splice site acceptor	Het
36	9	FPGS	ENST00000393706	Nonsynonymous	Het
37	9	AK1	ENST00000223836	Nonsynonymous	Het
38	9	FBXW5	ENST00000433269	Nonsynonymous	Het
39	10	ERCC6	ENST00000355832	Synonymous	Het
40	10	PDLIM1	ENST00000329399	Synonymous	Het
41	11	PYGM	ENST00000540450	Synonymous	Het
42	11	BATF2	ENST00000534177	Nonsynonymous	Het
43	11	SART1	ENST00000542816	Nonsynonymous	Het
44	11	USP35	ENST00000529308	Synonymous	Het
45	12	KRT75	ENST00000252245	Nonsynonymous	Het
46	13	DACH1	ENST00000377826	Synonymous	Het
47	13	LIG4	ENST00000442234	Nonsynonymous	Het
48	14	C14orf21	ENST00000396802	Nonsynonymous	Het

49	14	ACOT2	ENST00000238651	Nonsynonymous	Het
50	14	STON2	ENST00000557055	Nonsynonymous	Het
51	14	KIF26A	ENST00000423312	Synonymous	Hom
52	14	KIF26A	ENST00000423312	Nonsynonymous	Het
53	15	HERC1	ENST00000443617	Synonymous	Het
54	15	NPTN	ENST00000545878	Synonymous	Het
55	15	CLK3	ENST00000454830	Synonymous	Het
56	15	NTRK3	ENST00000540489	Synonymous	Het
57	16	WDR90	ENST00000549091	Nonsynonymous	Het
58	16	METRN	ENST00000219542	Synonymous	Het
59	16	MSLNL	ENST00000543963	Synonymous	Het
60	16	BAIAP3	ENST00000426824	Synonymous	Hom
61	16	PAQR4	ENST00000318782	Nonsynonymous	Het
62	16	IRX3	ENST00000329734	Nonsynonymous	Het
63	16	CNOT1	ENST00000546037	Synonymous	Het
64	16	HYDIN	ENST00000393567	Synonymous	Het
65	17	C17orf63	ENST00000452648	Synonymous	Het
66	17	HSD17B1P1	ENST00000442612	Nonsynonymous	Het
67	17	ARMC7	ENST00000245543	Synonymous	Het
68	18	LOXHD1	ENST00000536736	Nonsynonymous	Het
69	18	CBLN2	ENST00000269503	Synonymous	Het
70	19	CELF5	ENST00000541430	Synonymous	Het
71	19	DEDD2	ENST00000336034	Nonsynonymous	Het
72	19	KIR3DL2	ENST00000326321	Nonsynonymous	Het
73	20	PANK2	ENST00000497424	Synonymous	Het
74	20	MAFB	ENST00000396967	Synonymous	Het

75	20	LAMA5	ENST00000252999	Nonsynonymous	Het
76	20	KCNQ2	ENST00000370224	Synonymous	Hom
77	22	TRMT2A	ENST00000444845	Synonymous	Het
78	22	THAP7	ENST00000399133	Nonsynonymous	Het
79	22	KIAA1671	ENST00000406486	Nonsynonymous	Het
80	22	KIAA1671	ENST00000406486	Synonymous	Het
81	22	RP3-402G11.5	ENST00000380903	Nonsynonymous	Het
82	22	ADM2	ENST00000395738	Synonymous	Het
83	22	ODF3B	ENST00000428989	Synonymous	Het
84	X	DHRSX	ENST00000444280	Stop gained	Het
85	X	KDM6A	ENST00000543216	Synonymous	Het

Control fibroblasts

No.	**Chr**	**Gene name**	**Transcript ID**	**Effect**	**Hom/Het**
1	3	LAMB2	ENST00000494831	Nonsynonymous	Het
2	5	ARAP3	ENST00000513878	Nonsynonymous	Het
3	6	LAMA2	ENST00000421865	Nonsynonymous	Het
4	8	ZFHX4	ENST00000521891	Synonymous	Hom
5	11	SCUBE2	ENST00000520467	Nonsynonymous	Het
6	11	PGM2L1	ENST00000298198	Nonsynonymous	Het
7	16	PKD1	ENST00000423118	Synonymous	Het
8	16	ATXN2L	ENST00000395547	Nonsynonymous	Het
9	17	LLGL2	ENST00000545227	Synonymous	Het
10	17	CCDC57	ENST00000392347	Synonymous	Het
11	22	TRIOBP	ENST00000417174	Nonsynonymous	Het
12	X	CSF2RA	ENST00000501036	Nonsynonymous	Het

UNC-93B$^{-/-}$ iPSC line C

No.	Chr	Gene name	Transcript ID	Effect	Hom/Het
1	1	ATAD3B	ENST00000378737	Nonsynonymous	Het
2	1	OR10J3	ENST00000332217	Nonsynonymous	Het
3	1	SELE	ENST00000367782	Nonsynonymous	Het
4	1	CEP350	ENST00000367607	Nonsynonymous	Het
5	1	FAM129A	ENST00000367511	Nonsynonymous	Het
6	1	FAM5C	ENST00000534846	Nonsynonymous	Het
7	1	CTSE	ENST00000361052	Nonsynonymous	Het
8	1	CAPN9	ENST00000366666	Nonsynonymous	Het
9	2	KCNK12	ENST00000327876	Synonymous	Het
10	2	MOGS	ENST00000452063	Nonsynonymous	Het
11	2	MOGS	ENST00000452063	Synonymous	Het
12	2	HOXD10	ENST00000249501	Synonymous	Het
13	3	SEC61A1	ENST00000464451	Nonsynonymous	Het
14	3	IGSF10	ENST00000282466	Nonsynonymous	Het
15	3	SOX2	ENST00000431565	Synonymous	Het
16	4	KLHL5	ENST00000546147	Nonsynonymous	Het
17	4	TMPRSS11D	ENST00000545541	Nonsynonymous	Het
18	4	LIN54	ENST00000506560	Nonsynonymous	Het
19	4	NR3C2	ENST00000511528	Nonsynonymous	Het
20	4	GRIA2	ENST00000507898	Synonymous	Het
21	5	DBN1	ENST00000393565	Synonymous	Het
22	6	NUP153	ENST00000537253	Nonsynonymous	Het
23	6	ZNF165	ENST00000377325	Nonsynonymous	Het
24	6	CUL7	ENST00000535468	Nonsynonymous	Het

25	6	PKHD1	ENST00000393616	Nonsynonymous	Het
26	7	PAXIP1	ENST00000404141	Synonymous	Het
27	8	NKX6-3	ENST00000524115	Synonymous	Het
28	8	PKIA	ENST00000518467	Synonymous	Het
29	8	PKIA	ENST00000518467	Synonymous	Het
30	9	PPAPDC2	ENST00000381883	Nonsynonymous	Het
31	9	ADAMTSL1	ENST00000380566	Synonymous	Het
32	9	NPR2	ENST00000342694	Nonsynonymous	Het
33	9	PCSK5	ENST00000545128	Synonymous	Het
34	10	C10orf140	ENST00000449193	Synonymous	Het
35	10	ACSL5	ENST00000356116	Synonymous	Het
36	10	NRAP	ENST00000369360	Nonsynonymous	Het
37	10	MKI67	ENST00000537609	Nonsynonymous	Het
38	11	PIDD	ENST00000411829	Nonsynonymous	Het
39	11	OR52A4	ENST00000380369	Nonsynonymous	Het
40	11	OR52A4	ENST00000380369	Stop gained	Het
41	11	SF1	ENST00000433274	Synonymous	Het
42	11	KLHL35	ENST00000539798	Nonsynonymous	Hom
43	11	RPUSD4	ENST00000533628	Synonymous	Het
44	12	MLL2	ENST00000301067	Synonymous	Het
45	13	RNF17	ENST00000381921	Synonymous	Het
46	14	SYNE2	ENST00000555002	Nonsynonymous	Het
47	14	SYNE2	ENST00000555002	Synonymous	Het
48	14	ESRRB	ENST00000556177	Synonymous	Het
49	15	TYRO3	ENST00000540218	Nonsynonymous	Het
50	15	MAPKBP1	ENST00000514566	Synonymous	Het

51	15	SPTBN5	ENST00000320955	Nonsynonymous	Het
52	15	MFAP1	ENST00000267812	Nonsynonymous	Het
53	16	RBL2	ENST00000262133	Synonymous	Hom
54	16	MAF	ENST00000393350	Synonymous	Het
55	17	TP53	ENST00000509690	Nonsynonymous	Het
56	17	SLC6A4	ENST00000401766	Nonsynonymous	Het
57	17	ICAM2	ENST00000449662	Synonymous	Het
58	18	SMAD7	ENST00000262158	Synonymous	Het
59	19	PCSK4	ENST00000300954	Nonsynonymous	Het
60	19	TRMT1	ENST00000437766	Nonsynonymous	Het
61	19	FOXA3	ENST00000302177	Nonsynonymous	Het
62	20	ID1	ENST00000376112	Nonsynonymous	Het
63	20	KCNQ2	ENST00000430658	Nonsynonymous	Het
64	22	KIAA1671	ENST00000406486	Synonymous	Het
65	X	PTCHD1	ENST00000379361	Nonsynonymous	Het
66	X	DMD	ENST00000474231	Synonymous	Het
67	X	KDM6A	ENST00000543216	Synonymous	Het
68	X	SYTL4	ENST00000455616	Synonymous	Het
69	X	HNRNPH2	ENST00000457902	Synonymous	Het

UNC-93B$^{-/-}$ iPSC line H

No.	**Chr**	**Gene name**	**Transcript ID**	**Effect**	**Hom/Het**
1	1	IFFO2	ENST00000455833	Synonymous	Het
2	1	LRRC7	ENST00000370957	Nonsynonymous	Het
3	1	ZNF326	ENST00000394590	Nonsynonymous	Het
4	1	RBM15	ENST00000369784	Synonymous	Het
5	1	HIPK1	ENST00000443627	Synonymous	Het

6	1	BCL9	ENST00000234739	Nonsynonymous	Het
7	1	SELE	ENST00000367782	Nonsynonymous	Het
8	1	CEP350	ENST00000367607	Nonsynonymous	Het
9	1	FAM129A	ENST00000367511	Nonsynonymous	Het
10	1	FAM5C	ENST00000534846	Nonsynonymous	Het
11	1	CAPN9	ENST00000366666	Nonsynonymous	Het
12	2	ALK	ENST00000389048	Nonsynonymous	Het
13	2	BIRC6	ENST00000421745	Synonymous	Het
14	2	SIX3	ENST00000260653	Synonymous	Het
15	2	NRXN1	ENST00000536347	Synonymous	Het
16	2	BCL11A	ENST00000538214	Synonymous	Het
17	2	MOGS	ENST00000452063	Nonsynonymous	Het
18	2	MOGS	ENST00000452063	Synonymous	Het
19	2	TBR1	ENST00000389554	Synonymous	Het
20	2	FIGN	ENST00000333129	Synonymous	Het
21	2	DLX1	ENST00000469444	Synonymous	Het
22	2	HOXD10	ENST00000249501	Synonymous	Het
23	2	EIF4E2	ENST00000409322	Synonymous	Het
24	3	LHFPL4	ENST00000287585	Synonymous	Het
25	3	CACNA1D	ENST00000544977	Nonsynonymous	Het
26	3	MAGI1	ENST00000497477	Nonsynonymous	Het
27	3	SEC61A1	ENST00000464451	Nonsynonymous	Het
28	3	MSL2	ENST00000434835	Nonsynonymous	Het
29	3	FOXL2	ENST00000542203	Synonymous	Het
30	3	IGSF10	ENST00000282466	Nonsynonymous	Het
31	3	SOX2	ENST00000431565	Synonymous	Het

32	4	PCDH7	ENST00000543491	Synonymous	Het
33	4	KLHL5	ENST00000546147	Nonsynonymous	Het
34	4	ATP8A1	ENST00000264449	Synonymous	Het
35	4	TMPRSS11D	ENST00000545541	Nonsynonymous	Het
36	4	LIN54	ENST00000506560	Nonsynonymous	Het
37	4	NR3C2	ENST00000511528	Nonsynonymous	Het
38	5	UBE2QL1	ENST00000399816	Synonymous	Het
39	5	ISL1	ENST00000511384	Synonymous	Het
40	5	KCNN2	ENST00000512097	Synonymous	Het
41	5	SNX2	ENST00000514949	Synonymous	Het
42	5	MATR3	ENST00000510056	Synonymous	Het
43	5	NRG2	ENST00000544729	Synonymous	Het
44	5	PPARGC1B	ENST00000403750	Synonymous	Het
45	5	ODZ2	ENST00000545108	Synonymous	Het
46	6	NUP153	ENST00000537253	Nonsynonymous	Het
47	6	OR5V1	ENST00000543825	Nonsynonymous	Het
48	6	DDX39B	ENST00000458640	Synonymous	Het
49	6	ZBTB22	ENST00000431845	Nonsynonymous	Het
50	6	CUL7	ENST00000535468	Nonsynonymous	Het
51	6	TTBK1	ENST00000393984	Nonsynonymous	Het
52	6	TTBK1	ENST00000393984	Synonymous	Het
53	6	PKHD1	ENST00000393616	Nonsynonymous	Het
54	6	SYNCRIP	ENST00000369622	Synonymous	Het
55	6	CITED2	ENST00000537332	Nonsynonymous	Het
56	6	CITED2	ENST00000537332	Synonymous	Het
57	7	NEUROD6	ENST00000297142	Synonymous	Het

58	7	MAGI2	ENST00000536571	Synonymous	Het
59	7	LHFPL3	ENST00000543266	Synonymous	Het
60	7	PAXIP1	ENST00000404141	Synonymous	Het
61	8	NKX6-3	ENST00000524115	Synonymous	Het
62	8	MAFA	ENST00000333480	Synonymous	Het
63	9	NPR2	ENST00000342694	Nonsynonymous	Het
64	9	CDK5RAP2	ENST00000345313	Splice site acceptor	Het
65	9	RC3H2	ENST00000423239	Synonymous	Het
66	9	ZBTB26	ENST00000373656	Synonymous	Het
67	10	ZMYND11	ENST00000509513	Nonsynonymous	Het
68	10	C1QL3	ENST00000448557	Synonymous	Het
69	10	EPC1	ENST00000319778	Synonymous	Het
70	10	KCNMA1	ENST00000457953	Synonymous	Het
71	10	NRAP	ENST00000369360	Nonsynonymous	Het
72	10	MKI67	ENST00000537609	Nonsynonymous	Het
73	11	PIDD	ENST00000411829	Nonsynonymous	Het
74	11	STIM1	ENST00000533977	Synonymous	Het
75	11	OR52A4	ENST00000380369	Nonsynonymous	Het
76	11	OR52A4	ENST00000380369	Stop gained	Het
77	11	RBM14	ENST00000393979	Synonymous	Het
78	11	RBM14	ENST00000393979	Splice site donor	Het
79	11	RPUSD4	ENST00000533628	Synonymous	Het
80	12	CHD4	ENST00000544484	Synonymous	Het
81	12	LRP6	ENST00000543091	Synonymous	Het
82	12	MLL2	ENST00000301067	Synonymous	Het
83	12	TMTC2	ENST00000548305	Synonymous	Het

84	12	ATXN2	ENST00000550104	Synonymous	Het
85	13	SHISA2	ENST00000319420	Synonymous	Het
86	13	PCDH8	ENST00000448969	Synonymous	Het
87	13	DACH1	ENST00000377826	Synonymous	Het
88	13	SLITRK1	ENST00000377084	Synonymous	Het
89	13	ZIC5	ENST00000397451	Synonymous	Het
90	13	FAM155A	ENST00000375915	Synonymous	Het
91	13	SOX1	ENST00000330949	Synonymous	Het
92	13	SOX1	ENST00000330949	Synonymous	Het
93	14	NOVA1	ENST00000549146	Synonymous	Het
94	14	FOXG1	ENST00000382535	Synonymous	Het
95	14	FOXG1	ENST00000382535	Nonsynonymous	Het
96	14	NKX2-1	ENST00000354822	Synonymous	Het
97	14	SYNE2	ENST00000555002	Nonsynonymous	Het
98	14	SYNE2	ENST00000555002	Synonymous	Het
99	14	YLPM1	ENST00000423680	Synonymous	Het
100	14	ESRRB	ENST00000556177	Synonymous	Het
101	14	ZC3H14	ENST00000555900	Synonymous	Het
102	14	ZC3H14	ENST00000555900	Nonsynonymous	Het
103	15	TYRO3	ENST00000540218	Nonsynonymous	Het
104	15	MAPKBP1	ENST00000514566	Synonymous	Het
105	15	ARIH1	ENST00000299305	Nonsynonymous	Het
106	15	KIF7	ENST00000394412	Synonymous	Het
107	15	NR2F2	ENST00000394166	Synonymous	Het
108	16	FBXL19	ENST00000380310	Synonymous	Het
109	16	ZNF423	ENST00000535559	Synonymous	Het

110	17	TP53	ENST00000509690	Nonsynonymous	Het
111	17	C17orf63	ENST00000452648	Synonymous	Het
112	17	SLC6A4	ENST00000401766	Nonsynonymous	Het
113	17	NR1D1	ENST00000246672	Nonsynonymous	Het
114	17	WNT3	ENST00000225512	Nonsynonymous	Het
115	17	WNT3	ENST00000225512	Synonymous	Het
116	17	HOXB5	ENST00000239151	Synonymous	Het
117	17	LUC7L3	ENST00000393227	Synonymous	Het
118	17	SOX9	ENST00000455872	Synonymous	Het
119	18	MBD2	ENST00000398398	Synonymous	Het
120	19	TRMT1	ENST00000437766	Nonsynonymous	Het
121	19	EML2	ENST00000536630	Synonymous	Het
122	19	FOXA3	ENST00000302177	Nonsynonymous	Het
123	19	ASPDH	ENST00000389208	Nonsynonymous	Hom
124	20	PLCB1	ENST00000404098	Synonymous	Het
125	20	MAFB	ENST00000396967	Synonymous	Het
126	20	KCNQ2	ENST00000430658	Nonsynonymous	Het
127	22	KIAA1671	ENST00000406486	Synonymous	Het
128	X	PTCHD1	ENST00000379361	Synonymous	Het
129	X	IL1RAPL1	ENST00000378993	Synonymous	Het
130	X	KDM6A	ENST00000543216	Synonymous	Het
131	X	KDM6A	ENST00000543216	Synonymous	Het
132	X	KDM6A	ENST00000543216	Nonsynonymous	Het
133	X	PPP1R3F	ENST00000055335	Synonymous	Het
134	X	GPR173	ENST00000332582	Synonymous	Het
135	X	WNK3	ENST00000375169	Nonsynonymous	Het

136	X	AMMECR1	ENST00000372059	Synonymous	Het
137	X	RAB33A	ENST00000257017	Synonymous	Het
138	X	FHL1	ENST00000394155	Nonsynonymous	Het
139	X	FMR1	ENST00000440235	Synonymous	Het
140	X	RAB39B	ENST00000369454	Synonymous	Het

UNC-93B$^{-/-}$ fibroblasts

	Chr	**Gene name**	**Transcript ID**	**Effect**	**Hom/Het**
No.	1	AL359075.1	ENST00000464631	Nonsynonymous	Het
1	6	ATXN1	ENST00000450222	Nonsynonymous	Het
2	6	TRIM15	ENST00000376694	Synonymous	Het
3	7	GRID2IP	ENST00000435185	Splice site donor	Het
4	9	FAM163B	ENST00000496132	Synonymous	Het
5	17	DNAH17	ENST00000389840	Nonsynonymous	Het
6	X	AMOT	ENST00000524145	Nonsynonymous	Het

TLR3$^{-/-}$ iPSCs

No.	**Chr**	**Gene name**	**Transcript ID**	**Effect**	**Hom/Het**
1	1	YRDC	ENST00000373044	Nonsynonymous	Hom
2	1	HIPK1	ENST00000443627	Synonymous	Het
3	1	ILF2	ENST00000361891	Nonsynonymous	Het
4	2	SIX3	ENST00000260653	Synonymous	Het
5	2	PLA2R1	ENST00000392771	Nonsynonymous	Het
6	2	CHRNA1	ENST00000409542	Synonymous	Het
7	2	SPEG	ENST00000396698	Synonymous	Het
8	3	EOMES	ENST00000537516	Synonymous	Het
9	3	ARGFX	ENST00000334384	Nonsynonymous	Het

10	3	GATA2	ENST00000487848	Synonymous	Het
11	3	FXR1	ENST00000491062	Synonymous	Het
12	3	SOX2	ENST00000431565	Synonymous	Het
13	4	ODZ3	ENST00000511685	Synonymous	Het
14	5	CTNND2	ENST00000511377	Synonymous	Het
15	5	MATR3	ENST00000510056	Synonymous	Het
16	5	TLX3	ENST00000296921	Synonymous	Het
17	6	SRSF12	ENST00000452027	Nonsynonymous	Het
18	8	PXDNL	ENST00000543296	Nonsynonymous	Hom
19	8	RP1	ENST00000220676	Nonsynonymous	Het
20	8	GDF6	ENST00000454970	Nonsynonymous	Het
21	8	ATAD2	ENST00000287394	Nonsynonymous	Het
22	10	MINPP1	ENST00000371996	Nonsynonymous	Het
23	10	ENTPD1	ENST00000543964	Nonsynonymous	Het
24	10	ADRB1	ENST00000369295	Synonymous	Het
25	11	TRIM66	ENST00000402157	Nonsynonymous	Het
26	11	OR9G4	ENST00000302957	Synonymous	Het
27	14	REM2	ENST00000536884	Synonymous	Het
28	14	RGS6	ENST00000556437	Synonymous	Het
29	14	PAPOLA	ENST00000557320	Synonymous	Het
30	16	TFAP4	ENST00000204517	Nonsynonymous	Het
31	17	NLGN2	ENST00000302926	Synonymous	Het
32	20	MAP1LC3A	ENST00000397709	Nonsynonymous	Het
33	20	MAFB	ENST00000396967	Synonymous	Het
34	21	DSCAM	ENST00000404019	Synonymous	Het
35	X	NHS	ENST00000398097	Nonsynonymous	Het

TLR3$^{-/-}$ fibroblasts

	Chr	Gene name	Transcript ID	Effect	Hom/Het
No.	1	AHDC1	ENST00000374011	Nonsynonymous	Het
1	2	ARHGEF4	ENST00000409359	Nonsynonymous	Het
2	3	DCBLD2	ENST00000404023	Nonsynonymous	Het
3	6	NFKBIL1	ENST00000542852	Nonsynonymous	Het
4	6	GPSM3	ENST00000375043	Nonsynonymous	Het
5	7	RADIL	ENST00000544486	Nonsynonymous	Het
6	7	AUTS2	ENST00000406775	Nonsynonymous	Het
7	8	MTDH	ENST00000519934	Nonsynonymous	Het
8	11	LTBP3	ENST00000530866	Synonymous	Het
9	15	AC090098.1	ENST00000320930	Synonymous	Het
10	16	THAP11	ENST00000303596	Synonymous	Hom
11	17	SHMT1	ENST00000539052	Synonymous	Het
12	19	VASP	ENST00000245932	Synonymous	Hom

Suppl. Table 4. Fold-change expression data comparing glial and rosette stage cells

A) Oligodendrocytes

Probeset ID	*p*-value	Fold-change
OLIG1	9.25E-05	101.529
OLIG2	8.12E-07	100.273
APOD	1.60E-09	30.5307
FAM107A	0.00603635	28.5284
NKX6-2	0.00162927	17.3379
SCG2	0.0113763	16.6576
ANGPTL2	5.11E-06	15.9499
FAM5C	0.00134073	14.3401
S100A16	0.0169086	14.3157
FBXO32	0.00338735	13.2405
IFIT2	0.0071538	13.1046
LRRC3B	0.0108434	11.5217
NCAM2	0.00170106	11.4497
NKX2-2	0.0012738	11.0907
HS.557245	0.00106805	9.88082
NEU4	6.89E-13	9.76081
IFI44L	0.0490481	9.63491
CPNE4	0.000285552	9.30938
PTPRZ1	0.00905818	9.14412
C13ORF15	0.0175017	8.91703
DLL3	0.00701895	8.80436
C4ORF18	0.00886723	8.78147

NTRK2	0.000169104	8.44403
CBR3	0.000316533	7.9893
VCAM1	0.0100484	7.83027
FOSB	0.0151363	7.7322
AGT	0.0147416	7.05625
CHST7	0.00495793	6.98356
IGSF1	1.31E-06	6.9813
PLP1	0.000859161	6.96976
GLT25D2	0.0149425	6.88383
PAQR8	0.00269474	6.86416
SHD	0.00111939	6.82636
RGMA	0.0139014	6.71395
FERMT1	1.42E-05	6.5888
CADM2	0.00198303	6.40753
TGFB2	0.0101403	6.3671
LOC387683	1.83E-08	6.35476
THBS2	0.000481682	6.28254
ZCCHC24	0.0150545	6.25781
PPP1R16B	0.00365888	6.25147
ACOX2	0.0250373	6.22504
PITPNC1	8.97E-08	6.12531
KCNJ16	1.95E-07	6.03873
ADAMTS3	0.00318395	5.83543
LRIG1	0.00115833	5.64456
SLITRK2	0.00315307	5.61253
MT2A	0.00496038	5.60193

ENKUR	0.000437193	5.57016
COL20A1	5.08E-09	5.55422
OSBPL5	1.73E-05	5.51981
TMEM100	0.000721127	5.41546
SOX10	2.48E-12	5.36065
PLLP	0.000367519	5.34032
DOCK10	0.0273465	5.16118
ADORA2B	0.0149	5.08159
PCDH17	0.0425718	4.9975
SOX9	0.0480759	4.8917
C1QTNF5	0.0200012	4.80398
FLJ14213	0.0153598	4.79227
ADAMTS6	0.000255135	4.77526
NDRG2	0.00226906	4.74167
BCAS1	1.63E-16	4.71722
PDE4B	0.00101978	4.69186
SAMD9	0.00857704	4.67529
EDNRB	0.00892825	4.6718
RASL12	7.53E-05	4.54816
CHST9	0.00197748	4.50338
HS.576533	0.0021342	4.48207
HS.518794	0.00671485	4.43985
RAMP1	0.0115904	4.41404
PPP1R3C	0.0362624	4.33996
ACCN2	0.00265763	4.33494
MT1A	0.0143976	4.24297

CD9	0.0457264	4.23502
SLC15A2	0.00342969	4.19856
GPR137B	0.00303853	4.17504
SCD5	0.0250978	4.03682
MAG	4.20E-18	4.01088
WSCD1	0.0279755	4.00743
MGC16121	0.039749	3.99948
OPHN1	0.000366575	3.95133
EGFR	6.54E-07	3.93821
SH3PXD2B	0.00212287	3.91371
HS.571502	0.00284148	3.91229
KLHL4	0.0022517	3.85871
ASS1	0.0407322	3.80477
SEPP1	0.00244276	3.64026
ST3GAL5	0.013745	3.60573
DSEL	5.26E-08	3.5923
GALNT13	0.000174256	3.58605
KLF2	0.0290107	3.58258
HS.543067	0.000694736	3.58064
HS.493592	0.0138214	3.5747
SSPN	0.0291267	3.54667
CCND3	0.0024428	3.53692
EPN2	0.00229523	3.51679
ELFN2	0.0190794	3.47553
NOVA1	0.00253326	3.46155
HS.157613	8.93E-07	3.4516

LRRC8D	0.000892456	3.43671
CDH15	1.75E-07	3.42352
ANGPTL4	0.0404165	3.35295
FLJ11235	0.00316333	3.34071
CST3	0.0249805	3.30934
HS.546710	1.92E-07	3.29301
RLBP1	3.79E-08	3.29283
LOC644571	1.16E-07	3.29023
ZFP36L2	0.0251129	3.27755
PLD5	0.0417505	3.27322
SORL1	0.0380233	3.26733
VGLL3	0.0403673	3.23012
SPTAN1	0.000707738	3.22921
GPR17	4.64E-12	3.22538
NPAS3	0.0241259	3.20812
CDC42EP4	0.00959412	3.20628
MTTP	0.04925	3.19926
TNFRSF14	0.000135081	3.19755
MGC42367	0.0318031	3.18389
PSMB9	0.0230213	3.12327
HS.134779	1.54E-05	3.07092
GABBR1	0.0170772	3.05318
ABHD4	0.0019461	3.04721
CXCL16	0.00426318	3.00609
GRIA4	3.88E-06	3.00022
ZFPM2	0.014102	3.00018

KCNIP3	5.17E-07	2.9966
WFDC1	6.08E-05	2.96731
SH3D19	0.0275976	2.95075
TBC1D16	0.000239276	2.90117
ENPP6	1.45E-08	2.8991
LRP1B	0.0126732	2.87842
FIBP	1.97E-05	2.82438
PDSS1	0.00290252	2.82384
HS.423734	0.0038446	2.82343
ZNRF3	0.0360515	2.79769
MAN2B2	0.0369264	2.79349
MMP28	1.54E-05	2.79041
ELOVL1	0.0203222	2.78617
POLE4	8.13E-05	2.78511
RAPGEF4	0.00208419	2.77834
FAM59B	0.0493688	2.76818
HS.573264	0.00546008	2.75873
MAEL	2.20E-06	2.74366
NAGPA	0.000782983	2.74239
B3GALTL	0.0419335	2.72839
CRIPT	0.000184327	2.71958
DDR1	0.0223777	2.69648
FIBIN	0.0142413	2.68526
SP110	0.0310238	2.68467
KCNS1	0.000954313	2.6823
TRAF3IP2	0.0107732	2.66705

WDR21A	0.0463735	2.65933
MDGA2	0.0125411	2.65337
ZNF365	0.00396962	2.65011
DAG1	0.0347291	2.64376
ALG13	0.0131881	2.64271
GNA12	0.0095578	2.63904
UBL3	0.0462361	2.62518
C1ORF122	0.0012034	2.62516
HS.554391	9.72E-09	2.62259
RTKN	0.0239263	2.617
SLC6A11	5.83E-06	2.61129
PDZRN4	0.00667343	2.60886
WDR81	0.00624445	2.59859
TTYH2	0.00164888	2.59615
HS.159080	0.0303015	2.59268
HAPLN4	0.0326982	2.5824
LOC645236	0.041786	2.5803
ABHD3	0.0034179	2.56646
LOC643320	0.000351185	2.55452
SIK3	0.00638801	2.54948
MBP	0.0292151	2.5477
C8ORF46	0.0498513	2.53899
C10ORF65	0.00411516	2.53856
DLG5	0.0079372	2.53624
HS.556255	0.00296538	2.52835
ADCY8	0.00204732	2.51783

HCG22	3.26E-05	2.51668
SNX22	1.19E-05	2.5139
F8A1	0.00355357	2.51188
HS.25318	0.0154508	2.5101
MOSC1	0.0436842	2.50927
HS.50125	0.000147766	2.50414
C1ORF188	0.0121533	2.48725
RGR	8.14E-06	2.48172
LAMP1	0.00876089	2.47919
ACTN2	0.0024921	2.47553
PLCD4	0.00191206	2.47441
FOXRED2	0.00612248	2.4649
NPNT	0.00103905	2.45756
NTRK3	0.0278773	2.45568
DPP7	0.0252758	2.44493
NDUFC2	0.00242496	2.44219
PSMB10	0.0152355	2.41961
POLR2L	0.00878535	2.41824
DGCR2	0.0483704	2.41365
FAM120A	0.00232739	2.39403
COMMD4	0.0132721	2.39397
LOC441019	0.0120402	2.3907
MRPS18A	0.00125513	2.38397
DEGS1	0.00289237	2.37398
ATP2C2	8.27E-06	2.372
LOC644366	0.0145314	2.37109

PTRH1	0.013145	2.36105
ERMAP	0.00189066	2.35875
ANKRD57	0.0012729	2.3518
HGD	1.76E-07	2.3439
FAM102A	0.000681359	2.33767
PDE3A	1.16E-08	2.33403
LOC150356	0.000560474	2.32851
GRAMD3	0.0384994	2.328
HAP1	0.00210244	2.32353
VAX2	0.00759033	2.31743
PAQR7	0.00577843	2.31671
DOLK	0.0212527	2.31209
VPS8	0.00165392	2.306
ALDH9A1	2.17E-05	2.30348
MAML2	0.00996887	2.30139
SEPX1	0.0274688	2.29839
C19ORF70	0.0230888	2.29714
CENPB	0.0409693	2.2964
C9ORF156	3.96E-05	2.2862
ST7OT1	0.0208644	2.28312
SPNS1	4.01E-06	2.2791
MTG1	0.000462569	2.27875
ZDHHC14	0.00475427	2.26914
B3GAT2	0.000286094	2.26121
IGDCC4	0.047501	2.25387
DNLZ	0.00201715	2.25272

DAPK2	0.00126439	2.24832
LRRTM3	0.00124821	2.24751
MYO5A	0.013365	2.24666
NR1H3	0.0395649	2.24028
CD34	0.0363322	2.24
HS.535360	0.00473751	2.23964
C9ORF103	0.0265181	2.23455
PHKG1	1.49E-06	2.22705
MRPL24	0.0160917	2.22615
URM1	0.00111259	2.22163
PPP1R1C	0.00111862	2.21776
HPR	4.12E-10	2.21527
SLC9A9	0.00112882	2.2139
HECTD3	0.00128484	2.21273
WDR45	0.000211013	2.20724
SGPL1	0.000127936	2.20472
NDUFB2	0.00275256	2.20453
PHLPP1	0.00704766	2.20072
RPP40	0.0251999	2.19748
POLR2F	0.000705833	2.19688
FAM118B	0.000350228	2.19164
HADHA	0.00496991	2.19114
TTC15	1.33E-05	2.18429
ITPKA	0.0360723	2.18419
QKI	0.0290018	2.18329
LONRF1	0.00709257	2.17976

IL17RB	0.0430137	2.17755
HS.534096	0.00145375	2.1711
TMEM117	0.0444653	2.16828
SRPK3	1.44E-05	2.15285
TOB1	0.0381241	2.15091
CC2D2A	0.0103763	2.15063
ABCA9	2.93E-06	2.14305
KEAP1	0.0135922	2.13778
AGPAT5	0.0227101	2.13769
CHMP4A	8.95E-05	2.13661
OSTM1	0.000687168	2.13458
P2RX7	0.00358477	2.13431
ACYP2	0.0081243	2.1321
C9ORF114	0.0345359	2.12684
TNFSF12	0.00531462	2.12118
SLC40A1	0.00631144	2.11854
FLJ36070	0.00784945	2.1145
VPS45	0.00207339	2.10789
HNF4G	3.33E-05	2.10297
MEPCE	0.00057966	2.10241
SNX27	0.000254985	2.09733
C2ORF76	0.0014697	2.09696
LOC649801	0.028843	2.09603
HS.65839	0.00563057	2.09566
MAGED4B	0.000949105	2.09531
ENTPD1	0.00134996	2.09156

PPP2R5A	0.0319189	2.08859
HS.562110	0.0040296	2.08497
C16ORF7	0.0435033	2.08321
HS.553187	0.0273506	2.07656
UGT8	0.00173257	2.07489
DIRC2	0.0112026	2.07374
LRRC58	0.00799811	2.07192
C11ORF9	0.00882695	2.06997
FDX1L	0.00131286	2.06704
KIAA0494	0.0370062	2.06461
RAB5C	0.000652435	2.06456
CAPN3	1.62E-05	2.05899
OFD1	0.00800751	2.05754
RASSF4	0.0348358	2.05385
C17ORF82	6.24E-06	2.04462
FLJ20021	0.0113291	2.04009
CAMK2G	1.30E-05	2.03831
BDH2	0.00591055	2.03729
CYP2U1	0.0179187	2.03355
C2ORF27A	0.000198393	2.03335
CRELD2	0.00309741	2.03242
MED29	0.000352259	2.03238
UBXN8	0.0254385	2.03086
INPP1	0.0367323	2.02659
IL12A	0.0169293	2.02606
SH3GLB1	0.0231382	2.02235

PEPD	0.034008	2.01443
MOG	2.81E-06	2.01218
LMF1	0.0439784	2.01102
EAF2	0.0355112	2.00992
CLN3	0.000337906	2.00852
GPR172A	0.0303844	2.00366
RAPGEF1	0.00075171	2.00301
VPS18	0.0116934	2.003
CSNK1G2	0.0116974	-2.00103
ZSWIM4	0.00981746	-2.004
FIGN	0.00498295	-2.00594
LOC727751	0.00112139	-2.0074
SIRT4	0.0195615	-2.00889
HS.448059	0.000551575	-2.0094
RNF149	0.00701659	-2.01174
C10ORF47	0.00607555	-2.01377
ATP11C	0.0032172	-2.01786
LOC646168	0.0197967	-2.03164
STRC	2.02E-06	-2.03174
ASB12	9.77E-05	-2.03399
C6ORF130	0.0156557	-2.03842
ALKBH5	8.50E-06	-2.04278
LOXHD1	0.000285005	-2.04403
UVRAG	0.0165013	-2.04677
ERO1L	0.000793606	-2.05114
WWP1	0.0195543	-2.0616

YOD1	0.00346887	-2.06325
HS.559770	0.00410003	-2.06434
SLC27A2	0.0122725	-2.06481
LOC728411	0.0424063	-2.07166
YPEL2	0.0320155	-2.07292
WDR60	0.0175529	-2.07411
CNTNAP3B	0.0012993	-2.07566
PIGL	0.0162779	-2.0771
LOC91661	0.0111615	-2.07716
DNAH2	0.00127266	-2.08101
C9ORF126	0.0426065	-2.08235
PPARGC1A	0.0110371	-2.08283
HIT-40	0.0291636	-2.08405
CYP27C1	0.00121484	-2.0872
TNFAIP8L1	0.0361383	-2.08767
SERTAD2	0.0391906	-2.08957
GOLGA8A	0.0395935	-2.09368
NCK1	0.00570318	-2.09949
MRI1	0.00574948	-2.10139
ZNF219	0.0459233	-2.106
CEBPG	0.0445386	-2.10927
SLC9A5	0.0144796	-2.14787
MTFR1	0.0481356	-2.17399
HS.520591	0.000367204	-2.17514
EGLN1	0.027238	-2.17576
MBD2	0.0284908	-2.18805

POLB	0.00337407	-2.194
CTDSPL	0.00075442	-2.19582
FAM49A	0.0254794	-2.20238
AGTPBP1	0.00374226	-2.2057
DR1	0.00188236	-2.2184
LOC644128	0.026581	-2.22055
HS.547277	0.00469614	-2.23923
KCNJ12	0.000294973	-2.24272
LPCAT4	0.000628345	-2.25223
PDE7A	0.00517291	-2.25843
MSI1	0.00709711	-2.26881
CD46	0.000355741	-2.27975
RELL2	0.00839709	-2.28182
VANGL2	0.0465522	-2.2865
ZNF451	0.00115174	-2.2994
UCHL1	0.00738193	-2.30566
FKBP1B	0.0327188	-2.32319
USP53	0.00305445	-2.32412
MSX2	0.00939056	-2.32451
PLS1	0.0478984	-2.32869
KCNJ4	0.00108575	-2.33387
LNX2	0.000144742	-2.35414
KCTD9	0.0118522	-2.35807
N4BP3	0.00386166	-2.35889
GFPT1	0.00132105	-2.36169
JMJD1A	0.0297894	-2.36657

SLC36A4	0.0139511	-2.37243
SFRS13B	0.000943723	-2.37591
ACTL6A	0.000382327	-2.37949
INTS8	0.000226543	-2.3928
JAG2	0.0110857	-2.41793
MGC18216	6.48E-05	-2.41927
MS4A8B	0.0458367	-2.41943
BTBD3	0.0465445	-2.43532
MAP3K9	0.0230349	-2.46015
ZBTB46	0.0458505	-2.48323
C14ORF4	0.0338396	-2.48614
MAP4K1	0.0434537	-2.48862
C11ORF47	1.78E-07	-2.49831
TIFA	0.0269361	-2.50159
NARF	0.0245554	-2.50261
TSPAN4	0.0135899	-2.53154
ZNF330	0.000643307	-2.53164
FAM69B	0.0166785	-2.53672
KIAA1324	0.00829083	-2.53729
F12	0.0338401	-2.55188
PLEKHA1	0.00688433	-2.55863
KIAA1467	0.00302519	-2.56523
HS.568479	0.0386942	-2.57494
LOC728452	0.0203549	-2.59794
TMEM2	0.0492569	-2.59948
ADAMTS7	0.0254338	-2.59954

B4GALT6	3.15E-05	-2.61298
LOC388494	0.043927	-2.61406
MYADM	0.038823	-2.61481
FAM59A	0.0116136	-2.61824
HS.556018	0.00532991	-2.67536
HIC2	0.0442079	-2.68748
TMEM74	0.0275344	-2.69658
FLJ22795	0.00128735	-2.78184
PHIP	0.00912665	-2.78377
PAPSS2	0.0382878	-2.79312
PLCG2	0.0463073	-2.79514
KCNMB4	0.0328588	-2.84478
TMEM130	0.0218618	-2.85272
BASP1	0.0382806	-2.88582
SLC25A36	0.000748245	-2.89564
HS.538861	0.00866464	-2.91183
KIAA0895	0.032197	-2.98169
SLC29A3	0.00405512	-3.0149
CACNA1H	0.0421761	-3.01744
LPIN1	0.00128247	-3.0765
KISS1R	0.0318304	-3.08319
PIM1	0.0394346	-3.08783
TSC22D3	0.0115287	-3.09829
TBC1D9	0.0311841	-3.19096
PACSIN1	0.02188	-3.19194
PCK2	0.0433592	-3.23185

PREP	0.000240519	-3.24953
IGFBP2	0.0269581	-3.27518
LOC653344	0.00388699	-3.41496
TMEM88	0.0035325	-3.46285
KLHL3	0.0105631	-3.53969
LOC400406	0.0200501	-3.54641
DNAJA4	0.039963	-3.62946
ROD1	2.66E-05	-3.69593
CD83	0.00373044	-3.73489
IL11RA	0.00944154	-3.75385
WDR86	0.0400003	-4.01097
JARID2	0.0159137	-4.04305
C10ORF35	0.0209646	-4.28768
PRRT2	0.00155416	-4.31773
FLRT2	0.0173201	-4.9324
HS.137274	0.0018824	-5.10977
ARID3A	0.0100926	-5.17496
JUP	0.000519663	-5.44576
SEZ6L2	0.0130687	-5.66748
MIAT	0.0268865	-5.95144
ZNF558	0.0079276	-5.97868
REM2	0.0148874	-6.16244
PCDHB5	0.0137096	-6.35218
FBN2	0.0174373	-6.81214
TSHZ2	0.0228563	-7.06524
DUSP6	0.00524751	-7.2336

TFAP2C	0.00879396	-7.52966
IGSF21	0.0371087	-7.54059
FBLN1	0.0037725	-8.81554
STC2	0.0374311	-8.87065
LMO3	0.0418667	-9.21099
BEX2	0.0267527	-9.25593
SYT13	0.0490206	-10.4285
ALPL	0.00504025	-14.7487
STMN2	0.0215016	-51.8557

B) Astrocytes

Probeset ID	*p*-value	Fold-change
A2M	0.00744422	56.8967
GFAP	0.0148601	40.4864
CD44	0.0248124	29.1963
CAPN5	3.51E-06	24.4543
C1QL1	0.00920762	22.6696
SYNM	0.00147902	12.9679
HS.204481	0.00847691	10.7017
MAN1C1	0.00455299	10.6372
IFI16	0.0182172	10.4749
GAD1	0.0328599	10.0463
PLCH2	0.0452698	10.0228
SLC47A2	0.000841806	9.98104
RASD1	0.0187172	8.93283

CFI	0.0164621	8.76872
C21ORF62	0.0166782	8.14944
CDKN1A	0.00817105	8.12452
SIK1	0.000296215	6.95357
HS3ST3A1	0.0415969	6.62482
ZNF436	0.00218616	6.25592
SEPT5	0.0261995	6.24743
METTL7B	0.0176002	6.01326
RFTN1	0.0245109	5.96816
NTN1	0.035107	5.66477
LOC648256	0.0416742	5.60352
AP1S2	0.00597848	5.35666
ANGPT1	0.0108217	5.34854
B2M	0.0191145	5.25815
ZFP36	0.0429054	5.14805
DHRS3	0.0356295	4.98468
PLCD3	0.0260121	4.9428
PLCE1	0.0367825	4.80394
ADORA1	0.0313097	4.61886
CHL1	0.019655	4.56957
C19ORF4	0.0498638	4.56331
TMPRSS5	0.000733954	4.38291
ALK	0.0306266	4.176
HS.371609	0.0180365	4.0658
HS.543076	0.0306333	4.05194
APP	0.00545355	4.01134

CDCA7L	0.00946097	3.98166
PSRC1	0.0284438	3.90488
TP53I11	0.00101033	3.83794
IRS2	0.0307132	3.83247
RASD2	0.00719862	3.78824
KIAA1545	0.0131975	3.76059
RGL1	0.0155085	3.75393
MAP1A	0.0219089	3.7427
GPR37	0.0384487	3.73272
ARC	0.0457629	3.71
TIMP2	0.0179139	3.64771
FILIP1L	0.00287482	3.62644
LHFP	0.0488803	3.61376
SOCS3	0.0101283	3.45294
RNF180	0.0011392	3.45198
LOC646332	3.59E-05	3.44979
PLEKHH2	0.00260225	3.44906
TCF12	0.00695513	3.43548
DACT2	0.0159493	3.42863
LOC643169	0.0117059	3.41516
DRAM1	0.0304152	3.41283
CLASP2	0.0344396	3.33711
PTP4A3	0.00364599	3.28222
GPR88	0.00178426	3.2776
PLXNA3	0.0047638	3.25466
FXYD7	0.00343761	3.23621

FZD5	0.00707026	3.22863
EPHX1	0.0394188	3.22614
MYO5B	0.000710179	3.19048
KLF13	0.00302579	3.18721
RNF19A	0.0258032	3.17826
MARCH3	0.0168629	3.16992
SOCS2	0.00722712	3.16301
TGFB1I1	0.0453181	3.14843
ENAH	0.00858364	3.12698
SHC2	0.00188026	3.11855
HS.22689	0.0218623	3.08373
UAP1L1	0.0475672	3.08325
HS.184721	0.0132258	3.08172
GAS7	0.0288612	3.02678
PSCD1	0.00102248	2.98667
HS.193767	0.00843577	2.97699
HRK	0.0153333	2.97446
ETV6	0.0134162	2.96587
PCDH8	0.0264653	2.90768
MAP3K1	0.0102233	2.89344
KIAA0802	0.000929403	2.88655
PDE8B	0.0466464	2.87622
KLHL20	0.0410508	2.86518
SLC26A7	0.00128212	2.85855
SFRP4	0.044028	2.84901
HS.57079	0.000666251	2.82035

PLEKHG4B	0.0192389	2.81059
C6ORF59	0.0286393	2.79445
CARS	0.00742781	2.7731
ACPL2	0.0437612	2.76351
TLE6	0.000177263	2.76314
TRPM8	0.0173793	2.74557
HS.561493	0.0376267	2.73956
TP53INP1	0.00642946	2.73067
ZBTB4	0.0216213	2.72792
NRIP1	0.0163558	2.70875
HS.143018	0.00410079	2.68187
MC1R	0.000752345	2.66438
EFTUD2	0.0434009	2.65455
APBB3	0.0305292	2.65094
HS.568945	0.000881213	2.63661
ATG4A	0.0193152	2.62232
NCOR2	0.00496434	2.62135
GDPD2	0.0300711	2.61565
TRIM69	0.00913029	2.60935
DDIT3	0.018403	2.60848
ITGA7	0.0106187	2.58169
HS.128848	0.000250453	2.57553
BEX1	0.0290618	2.57518
C19ORF18	0.00526613	2.56777
DIP2C	0.0199542	2.55622
ONECUT2	0.0160906	2.54887

GAL3ST4	0.0417959	2.53507
NADK	0.000218624	2.50769
LOC643505	0.000681809	2.49738
TMEM63A	0.0252175	2.49192
MMP15	0.0129372	2.4916
TMEM49	0.0251359	2.48543
HS.428370	0.0256186	2.48514
OSMR	0.036623	2.47695
LOC728014	0.0261817	2.47552
CLSTN2	0.0028795	2.47389
LYST	0.00759608	2.47036
LOC728734	0.00974408	2.45957
LONRF2	0.0143029	2.44842
KIAA0913	0.0204276	2.44407
APEG1	0.00543285	2.42563
ZMAT3	0.0451844	2.41953
SGSM2	0.00895869	2.41906
C10ORF6	0.00674383	2.40176
HS.527515	0.00681668	2.36744
FAM135A	0.00248996	2.33678
LASS5	2.38E-06	2.32689
FTH1	0.0397671	2.3223
WDR91	3.05E-05	2.32032
ZAK	0.024697	2.31703
PIK4CA	0.0177557	2.31338
ZNFX1	0.0443597	2.30116

PPP1R1B	0.0454921	2.29264
PKD1	0.0112812	2.29168
POLN	0.00294993	2.28682
RP5-1022P6.2	0.0117891	2.28091
MAMDC4	0.0125222	2.26472
MAGI2	0.0108476	2.25771
CLEC16A	0.00673328	2.25179
AMDHD2	0.0380019	2.25097
SUSD1	0.0358071	2.24755
HS.544679	0.0176384	2.24717
HKDC1	0.0166725	2.24627
CCDC106	0.00648363	2.24616
C12ORF5	0.0220172	2.24585
LOC220686	0.0317608	2.23491
ARFGEF1	0.00246669	2.22167
BICD1	0.0150916	2.21672
HS.537004	0.0463057	2.21233
GALIG	0.0234082	2.21222
CIC	0.00666413	2.19937
LRSAM1	0.00403892	2.19274
CASP6	0.0122341	2.18266
PPP1R10	0.00342833	2.17558
REPS1	0.00301183	2.16739
HS.559714	0.0136504	2.16721
RCVRN	0.00208787	2.16711
AGXT2L2	0.00218453	2.16603

ASCC2	0.000568475	2.15466
ALDH3A2	0.00176812	2.14549
LRRC16	0.00870684	2.13321
DAPK1	0.0411145	2.13013
ZNF621	0.00906444	2.1203
CRYGS	0.0256537	2.11273
SPON2	0.0303035	2.10429
ITPRIP	0.047244	2.10334
DCHS1	0.0335573	2.10281
HS.545585	0.00013175	2.09977
LOC654127	0.0166428	2.09954
LGALS12	1.29E-05	2.09573
PLCL4	0.0237848	2.09265
RERE	0.0149306	2.09014
WDR1	0.0270752	2.08829
CLDN15	0.000589847	2.08431
LOC390414	0.0232115	2.08241
PCSK7	0.00579137	2.08214
HS.56147	0.0139497	2.08205
RICS	0.0421931	2.08072
TSC22D2	0.0224498	2.07393
FLJ23834	0.0459375	2.07165
PIP4K2C	0.0132001	2.06933
NAGLU	0.0167181	2.06834
LRFN2	0.0369177	2.06361
AMY2A	0.0178938	2.06206

GLCCI1	0.0151999	2.06042
NADSYN1	0.0173195	2.04903
LCN9	0.000380098	2.04277
LOC652683	0.0222052	2.03955
SPTBN1	0.0160115	2.03883
MYO7A	2.10E-06	2.03406
PHLDB1	0.0145381	2.03376
LOC645850	0.00043253	2.03281
CYP21A2	0.0158794	2.02057
SPATA5L1	0.0326649	2.01361
PIP5K1C	0.0465276	2.01278
ZMIZ2	5.02E-05	2.00972
MARK3	0.00496026	2.00348
SNX19	0.000282863	2.00025
GPR63	0.00477863	-2.00468
C9ORF6	0.000259007	-2.00517
ZNF334	0.00910053	-2.00553
LRP11	0.0195786	-2.00587
STRBP	0.0435147	-2.01121
MVK	0.035556	-2.01461
PCDHB15	0.0226923	-2.01521
RALB	0.0416407	-2.01779
RAD9A	0.00249043	-2.02047
FAM171A1	0.0182405	-2.02396
TMEM177	0.0230446	-2.02458
TAF5	0.0167786	-2.02558

C10ORF82	0.00852192	-2.0373
SLC25A15	0.0223218	-2.03895
WDR57	0.0327061	-2.04156
LOC389203	0.0153534	-2.0452
LOC645058	0.0152089	-2.04682
FH	0.000154896	-2.049
PGRMC1	0.00622909	-2.04923
NUP107	0.00241149	-2.05406
ZBBX	0.000139674	-2.05603
PPIH	0.0125612	-2.05729
TRAF3	0.00351316	-2.06144
NINL	0.0167797	-2.06221
MTL5	0.00262937	-2.06285
AS3MT	0.000756715	-2.0647
TSP50	0.00012005	-2.06683
SYTL3	0.000453441	-2.06714
FBXO5	0.00817723	-2.06764
RBKS	0.00240036	-2.06771
STARD4	0.000354677	-2.07487
C10ORF57	0.0178486	-2.07513
SNRPB	0.0370499	-2.07514
C20ORF45	0.00870194	-2.07926
LIG1	0.0382464	-2.07956
LOC647954	0.0282156	-2.08437
WNT4	0.0144552	-2.08871
CDCA1	0.0329966	-2.09075

SMC2	0.040336	-2.09401
MORN5	5.93E-05	-2.09466
PSMC3IP	0.00579392	-2.10082
HSP90AB1	0.00206747	-2.10287
CRYGD	0.00130263	-2.11195
POLR2D	0.0330364	-2.11604
GOLPH3L	0.0027028	-2.11612
C1ORF229	0.00261418	-2.11889
WDR63	0.000553305	-2.1225
C7ORF68	0.0245749	-2.12768
MAOB	0.000282718	-2.128
LOC401152	0.00311447	-2.12877
CD164L2	0.00134933	-2.13426
SNRPF	0.0298721	-2.14228
HS.405877	0.00497919	-2.14336
CETN3	0.0152146	-2.15264
C13ORF30	3.76E-05	-2.15691
STAC	0.0392267	-2.19172
LOC143543	0.00440688	-2.19494
FANCD2	0.018547	-2.20114
PRKCABP	0.0246781	-2.2013
ARHGEF16	0.0211485	-2.20212
LRRIQ1	0.000379891	-2.20383
NOS3	0.0332881	-2.2095
KHDC1	0.0289325	-2.21929
HS.532698	0.032643	-2.22949

NUF2	0.00580439	-2.23297
AMMECR1	0.0295579	-2.23382
LSAMP	0.0318628	-2.24044
RTN4RL1	0.000323588	-2.24398
LOC646849	0.0379897	-2.25314
C1ORF218	0.0410531	-2.26215
CGB1	1.03E-09	-2.26443
BET1	0.00261394	-2.27836
NARS2	0.00203171	-2.27984
C9ORF40	0.0140613	-2.28827
SLFN12	0.0499795	-2.29989
ABCB4	0.00761486	-2.30075
CBLB	0.00716789	-2.30647
PKP4	0.0339337	-2.31162
CACNA1A	0.00074258	-2.31822
RFC4	0.0149179	-2.34367
HSD11B2	0.0386784	-2.35105
ARMCX2	0.000336769	-2.3694
GGH	0.0138206	-2.3705
LOC284023	0.0380921	-2.37302
LYL1	9.91E-05	-2.37825
ACBD7	0.0456511	-2.38119
HRASLS	0.0359031	-2.40019
ZCCHC3	0.0277919	-2.40279
NIF3L1	0.00231975	-2.42182
LOC650826	0.0224812	-2.42618

HAUS4	0.0256362	-2.44508
LOC440160	0.00680354	-2.44561
NXT2	0.00654227	-2.45065
C18ORF54	0.00585985	-2.45595
CXXC4	0.0488544	-2.46335
TMEM216	0.0371462	-2.4706
FADS1	0.0227982	-2.47447
CSRP2	0.0315696	-2.47972
LRRC8C	0.00468211	-2.47991
N6AMT2	0.00573743	-2.48533
UGDH	0.00952016	-2.51027
RACGAP1	0.0120911	-2.51233
PRIM1	0.0274539	-2.51253
SYT9	0.0184347	-2.51446
OPLAH	0.0189339	-2.5407
ANLN	0.0202664	-2.56555
CCDC58	0.00116803	-2.5739
CABYR	0.00369168	-2.57897
BCL2	0.0115373	-2.58304
CHAF1B	0.0452558	-2.62423
KIF18A	0.0020093	-2.62974
RFC5	1.68E-05	-2.64811
CETN2	0.0360394	-2.65761
LOC643287	0.0229567	-2.67447
CDC7	0.00936239	-2.68467
LOC728037	0.0309837	-2.70808

FAM127B	0.0145423	-2.73266
NDC80	0.0202288	-2.73291
ZIC1	0.0476825	-2.75171
NAALAD2	0.0202629	-2.75431
TUB	0.0462136	-2.76739
FANCI	0.0143767	-2.77452
CDC25A	0.0223721	-2.79217
C6ORF192	0.00556864	-2.82535
YEATS4	0.0249814	-2.82593
HS.567759	0.0190882	-2.85648
LRRN1	0.0466564	-2.86761
JAZF1	0.0259153	-2.89297
RPA3	0.0265949	-2.89828
NMRAL1	0.0445946	-2.91269
RNASEH2A	0.037893	-2.92394
CCNF	0.0488725	-2.92896
PCDH7	0.0170357	-2.92914
NDUFAF2	0.00114508	-2.93137
NUDT16	0.00090441	-2.94056
MND1	0.0111421	-2.97444
CHCHD6	4.55E-05	-2.98045
KIF11	0.04385	-3.03506
CDCA4	0.0353895	-3.05
DTL	0.0318987	-3.05245
ARL9	0.0443322	-3.09314
RAB11FIP4	0.0416076	-3.10343

PPAPDC3	0.00351671	-3.17622
TRIP13	0.0193468	-3.2313
CKAP2L	0.0458458	-3.23209
PPCS	0.0134703	-3.24027
PLIN2	0.00448052	-3.2568
C10ORF33	0.00778891	-3.25874
FDPS	0.000997701	-3.31246
RNASET2	0.00427521	-3.34289
KIF14	0.00255372	-3.35572
FZD9	0.0355917	-3.36038
UBE2T	0.0400664	-3.36567
CEP55	0.0249437	-3.42559
AHCY	0.0176768	-3.49037
UCP2	0.0115392	-3.53425
SCD	0.00699781	-3.54424
CENPN	0.0404844	-3.55355
IDI1	0.00170882	-3.5804
BIRC5	0.0490989	-3.63415
STAMBPL1	0.031645	-3.63622
FGFBP3	0.0416794	-3.64257
PHF11	0.0136003	-3.72949
OIP5	0.0242146	-3.73391
GINS2	0.0329271	-3.7496
APOC1	0.0272935	-3.75591
CENPA	0.00774439	-3.77898
ECT2	0.0164654	-3.80785

CNTN3	0.000331434	-3.8173
MELK	0.0407946	-3.82097
TYMS	0.0234463	-3.83665
ACAT2	0.00367761	-4.08583
DHCR24	0.000423426	-4.22154
NECAB2	0.0120314	-4.4167
CDCA8	0.0113126	-4.42129
RAD51AP1	0.00733908	-4.42835
FAM64A	0.0156121	-4.45508
HS.348844	0.0100661	-4.46926
CLDN11	0.0276058	-4.50741
SLC7A3	0.046768	-4.63481
ATIC	0.00236895	-4.68341
CDCA3	0.0203969	-4.72123
OPCML	0.0409118	-4.81216
FAM83D	0.00951948	-4.82407
H1F0	0.0490925	-4.8506
C6ORF173	0.0015	-4.99378
PNMA3	0.0254097	-5.2363
TOP2A	0.00681087	-5.4769
ODZ3	0.0138854	-5.72791
NR4A2	0.00239686	-7.33225
GALC	6.63E-06	-7.70992
GPX7	0.000413522	-8.45588
SH3GL3	0.0243212	-8.83361
RPRM	0.0219549	-9.70285

LPL	0.0317454	-10.0544
RBP1	0.00121436	-11.0637

Supplementary references

1 Park, I.H. *et al.*, Disease-specific induced pluripotent stem cells. *Cell* **134**, 877-886 (2008).

2 Barberi, T. *et al.*, Neural subtype specification of fertilization and nuclear transfer embryonic stem cells and application in parkinsonian mice. *Nat Biotechnol* **21**, 1200-1207 (2003).

3 Perrier, A.L. *et al.*, Derivation of midbrain dopamine neurons from human embryonic stem cells. *Proc Natl Acad Sci U S A* **101**, 12543-12548 (2004).

4 Somers, A. *et al.*, Generation of transgene-free lung-disease specific human iPS cells using a single excisable lentiviral stem cell cassette. *Stem Cells* **28**, 1728-1740 (2010).

5 Mostoslavsky, G., Fabian, A.J., Rooney, S., Alt, F.W., & Mulligan, R.C., Complete correction of murine Artemis immunodeficiency by lentiviral vector-mediated gene transfer. *Proc Natl Acad Sci U S A* **103**, 16406-16411 (2006).

6 Li, H. & Durbin, R., Fast and accurate short read alignment with Burrows-Wheeler transform. *Bioinformatics* **25**, 1754-1760 (2009).

7 McKenna, A. *et al.*, The Genome Analysis Toolkit: a MapReduce framework for analyzing next-generation DNA sequencing data. *Genome Res* **20**, 1297-1303.

8 Li, H. *et al.*, The Sequence Alignment/Map format and SAMtools. *Bioinformatics* **25**, 2078-2079 (2009).

9 Ying, S.W. & Goldstein, P.A., Propofol-block of SK channels in reticular thalamic neurons enhances GABAergic inhibition in relay neurons. *J Neurophysiol* **93**, 1935-1948 (2005).

10 Ying, S.W. *et al.*, Dendritic HCN2 channels constrain glutamate-driven excitability in reticular thalamic neurons. *J Neurosci* **27**, 8719-8732 (2007).

11 Park, I.H. *et al.*, Reprogramming of human somatic cells to pluripotency with defined factors. *Nature* **451**, 141-146 (2008).

12 Yang, K. *et al.*, Human TLR-7-, -8-, and -9-mediated induction of IFN-alpha/beta and -lambda Is IRAK-4 dependent and redundant for protective immunity to viruses. *Immunity* **23**, 465-478 (2005).

13 Lee, G. *et al.*, Modelling pathogenesis and treatment of familial dysautonomia using patient-specific iPSCs. *Nature* **461**, 402-406 (2009).

14 Sommer, C.A. *et al.*, Induced pluripotent stem cell generation using a single lentiviral stem cell cassette. *Stem Cells* **27**, 543-549 (2009).

15 Sommer, C.A. *et al.*, Excision of Reprogramming Transgenes Improves the Differentiation Potential of iPS Cells Generated with a Single Excisable Vector. *Stem Cells* **28**, 64-74 (2009).

16 Staerk, J. *et al.*, Reprogramming of Human Peripheral Blood Cells to Induced Pluripotent Stem Cells. *Cell Stem Cell* **7**, 20-24 (2010).

17 Park, I.H., Lerou, P.H., Zhao, R., Huo, H., & Daley, G.Q., Generation of human-induced pluripotent stem cells. *Nat Protoc* **3**, 1180-1186 (2008).